Early transcriptional changes in neutrophil-mediated processes following recanalization after ischemic stroke

Truong An Bui[1,2], Yonglie Ma[1], Glen C Jickling[2,3], Ian R Winship[1,2]
[1]Neurochemical Research Unit, Department of Psychiatry, Faculty of Medicine and Dentistry, University of Alberta, Edmonton, Alberta, Canada
[2]Neuroscience and Mental Health Institute, University of Alberta, Edmonton, Alberta, Canada
[3]Department of Medicine, Faculty of Medicine and Dentistry, University of Alberta, Edmonton, Alberta, Canada

Abstract

Background: Ischemic stroke is a leading cause of mortality and long-term disability globally. Current recanalization therapies, including mechanical thrombectomy and thrombolysis, aim to restore blood flow in acute ischemic stroke patients. However, many patients with successful recanalization still experience poor clinical outcomes. This phenomenon, where the restoration of blood flow does not translate into functional recovery, is known as futile recanalization.
Methods: Using a murine middle cerebral occlusion (MCAO) model that mimics a large vessel occlusion with recanalization, a comprehensive microarray analysis of gene expression from blood samples collected during MCAO and after recanalization (N=44) was performed.
Results: *Il1r2, Cd55, Mmp8, Cd14,* and *Cd69* were key regulatory genes expressed early after MCAO and recanalization. A comparison with gene expression data from human stroke patients and rat MCAO model (GSE16561 and GSE21136) revealed *Vcan* as a differentially expressed gene conserved across species, marking it as a novel indicator of recanalization that was detected as early as 3 hours post-recanalization (4 hours post-MCAO) in mice and 24 hours after recanalization rats (MCAO-thrombectomy) and humans (rtPA-thrombolysis). Leukocyte and neutrophil activation pathways were significantly enriched in the mouse data and human samples from GSE16561, with greater upregulation in female subjects. The analysis identified key miRNAs regulating gene expression in response to recanalization, and NFE4 and MTF1 as crucial transcription factors regulating these processes. Based on these data, a coregulatory network underlying neutrophil activity was constructed, highlighting its central role in early recanalization responses, especially in females.
Conclusions: This study identified new genomic markers in blood associated with recanalization, and identified critical age- and sex-specific factors. By mapping a coregulatory network of interacting genes and neutrophil-related pathways, the data provides insights to inform future research and develop targeted therapies. Such therapies can improve recanalization efficacy or modulate leukocytes to reduce futile recanalization, ultimately enhancing clinical outcomes for ischemic stroke patients.

Keywords: recanalization, ischemic stroke, biomarkers, neutrophil, peripheral response, reperfusion injury

Graphical Abstract

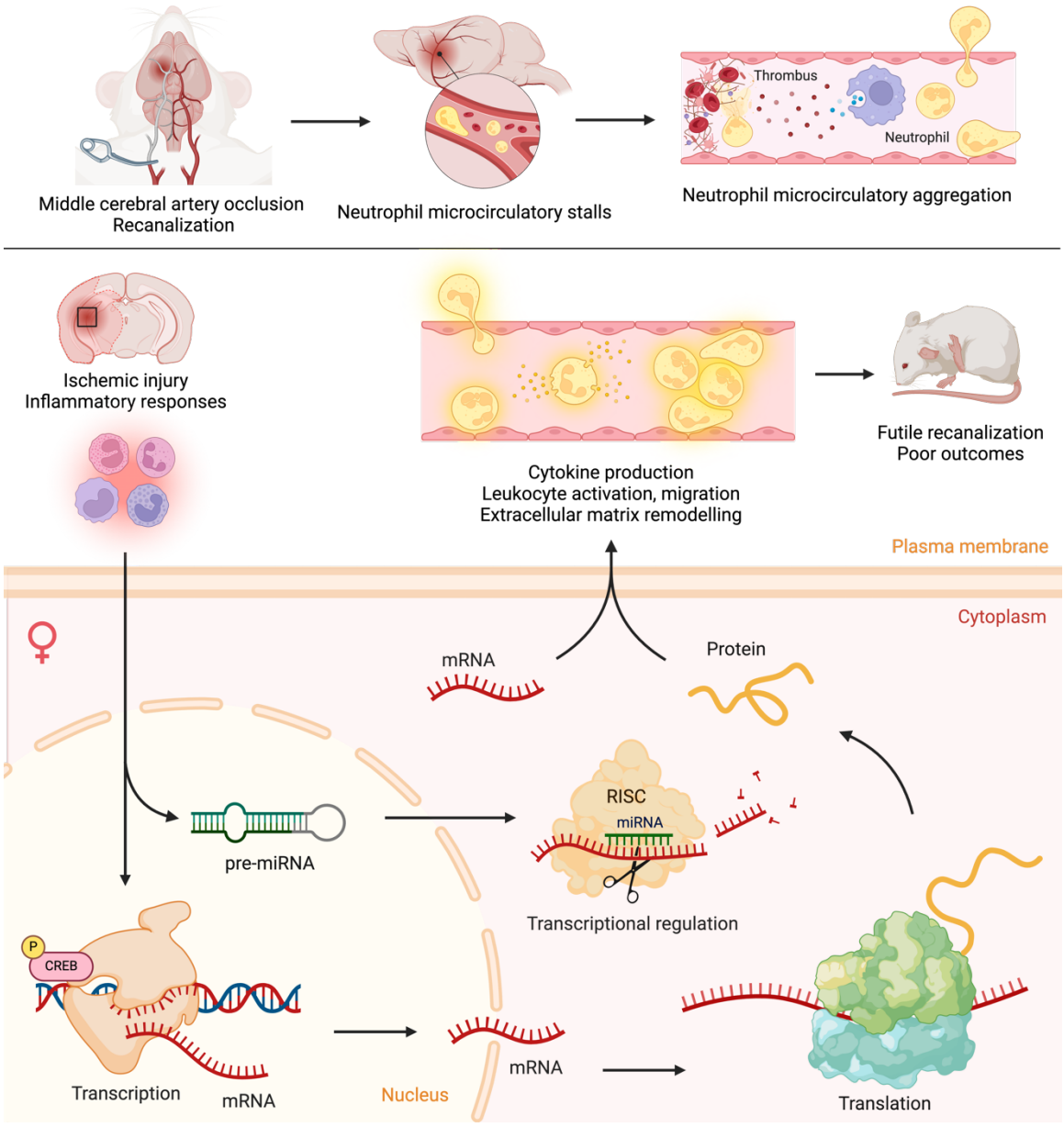

Introduction

In the 2021 Global Burden of Diseases, Injuries, and Risk Factors Study, stroke was identified as the third leading cause of mortality worldwide, following ischemic heart disease and COVID-19 (1). Ischemic stroke, the predominant subtype, accounts for approximately 75-80% of all stroke cases (2). It resulted in an estimated 3,870,000 deaths globally (1,3) and contributed to 160.4 million disability-adjusted life years (4). The epidemiology of stroke reveals a pronounced age-related incidence, predominantly affecting individuals aged 65 and older (2). Notably, there is a sex disparity in the age of onset, with women experiencing strokes 4 to 6 years later than men (5). However, women under 35 years old have a 44% higher likelihood of ischemic stroke relative to men (6). Overall, women have a greater lifetime risk of ischemic events and transient ischemic attacks (6). After middle age, the incidence and long-term risks of ischemic stroke rise more steeply in women, paralleled by an increase in the severity of resultant disabilities (7). This heightened risk with increasing age contributes to a significant public health challenge given the global demographic shifts towards aging populations (8).

The best available treatment for ischemic stroke is recanalization therapy via thrombolysis with tissue plasminogen activator (alteplase) or tenecteplase (9) and/or endovascular therapy (EVT) (10). While recanalization restores flow in the occluded vessel, restored flow does not always extend into the microcirculation that nourishes brain tissue. This can result from collateral failure, whereby cerebral ischemia in penumbral regions worsens over time due to the collapse of the collateral circulation (11). It also results from microcirculatory failure, where dysfunction in the small blood vessels within the brain tissue that impairs microcirculation even after the large vessel is recanalized (12). A key contributor to this dysfunction is the post-ischemic "stalling" of neutrophils within cerebral microvessels. Even after recanalizartion, neutrophils adhere to endothelial cells and aggregate in microvessels, preventing blood flow in microvessels, becoming activated and releasing pro-inflammatory cytokines, amplifying tissue damage, and driving further inflammation (for review, see (13)). Further, while the goal of recanalization is to restore blood flow, alleviate tissue hypoxia, and salvage ischemic tissue, restoration of flow can paradoxically cause tissue damage. This complication, known as reperfusion injury, and happens when blood flow is abruptly restored to previously ischemic tissue after a period of oxygen deprivation, causing a rush of molecular oxygen and leading to rapid reactive oxygen species production. This, in turn, causes oxidative stress, prolonged inflammation, activation of immune cells in the blood and brain, and can potentiate microcirculatory failure (14).

Although the success rate of recanalization has improved over time, many patients still experience poor long-term outcomes, as measured by the modified Rankin Scale (mRS) at 90 days and the National Institutes of Health Stroke Scale. This phenomenon, known as futile recanalization—where patients remain functionally dependent despite successful recanalization (mRS ≥ 3)—occurs in 32-57% of ischemic stroke patients who

undergo EVT (15,16) and is exacerbated by collateral failure, microcirculatory failure, and reperfusion injury (11,17).

Patterns of gene expression following ischemic stroke offer valuable insights into the underlying causes of reperfusion injury and potential outcomes of recanalization. Comparative analyses of gene expression profiles across different types of blood cells in stroke patients reveal that transcriptional alterations primarily occur in neutrophils (18). These transcriptional shifts are modulated by interactions between neutrophils, platelets, and cytokines, which may amplify the inflammatory response and impact stroke outcomes (13). This suggests neutrophils can be an early peripheral and genomic signature of post-recanalization microcirculatory failure (19). Changes in gene expression profiles may indicate ongoing inflammatory and repair processes, potentially serving as biomarkers to assess the severity and progression of stroke, as well as the risks and mechanisms of futile recanalization. Understanding the role of neutrophils in recanalization could guide the development of therapeutic strategies to prevent futile recanalization and improve patient outcomes. A rapidly measurable blood-based biomarker panel could also be invaluable for informing clinical decisions during initial triaging and acute care to reduce risks of futile recanalization.

This study explored early transcriptional changes occurring in peripheral blood following stroke with or without recanalization in a mouse model. Dynamic gene expression patterns were analyzed to uncover regulatory pathways responding to MCAO and recanalization. The analyses identified several critical genes that could serve as new biomarkers or predictors of ischemic/reperfusion injury following recanalization. Notably, sex- and age-specific differences in gene expression were observed, with female mice and aged mice displaying unique patterns of leukocyte and neutrophil-related gene activation. *Vcan* emerged as a novel biomarker for ischemic stroke and recanalization, and the only gene conserved across mice, rats, and humans. *Vcan*'s distinct expression in aged animals, especially as a central miRNA regulatory node, points to a previously unexplored aspect of ischemic stroke and reperfusion injury biology. Finally, a coregulatory network composed of rich interactions between identified differentially expressed genes, miRNAs, and their transcription factors in neutrophil-centred pathways linked to reperfusion injury, was compiled for the first time. These discoveries open new avenues for understanding the molecular mechanisms driving stroke recovery and may provide insights for developing therapies tailored to age and sex.

Methods

1. Middle cerebral artery occlusion (MCAO) surgery

Experimental methods are outlined in **Supplementary Figure 1**. Wild-type mice (C57BL6/J) in the University of Alberta Health Sciences Laboratory Animal Services facility were obtained and kept in a pathogen-free animal room at 18-22°C and 60% humidity with free access to food and water. Proximal middle cerebral artery occlusion

(MCAO) was modelled by transecting the external carotid artery, ligating the common carotid artery, and inserting a Doccol monofilament through the internal carotid artery to occlude the origin of the middle cerebral artery. Body temperature was monitored throughout the surgery using a rectal probe and maintained at 37.0 ± 0.5°C by a heating pad. The suture was placed for 60 minutes before removal to mimic complete recanalization.

Three experimental groups (N=44), sham (SHAM, N=16), 1-hour MCAO (MCAO, N=17), and 1-hour MCAO with 3-hour recovery post-recanalization (MCAO+Recan, N=11), were included in the dataset. Both young adult (3-6 months old, N=20) and aged (18-24 months old, N=24), male (N=20) and female (N=24) mice were used. MCAO mice were euthanized immediately 60 minutes after surgery. In the MCAO+Recan group, the suture causing MCAO was removed 60 minutes after the onset of occlusion and mice were allowed to recover for an additional 3 hours before euthanasia. SHAM mice were subjected to only anesthesia and the manipulation of surrounding tissues and arteries with 4 hours of recovery before sample collection.

All mice were anesthetized with an intraperitoneal injection of 20% urethane at the point of sample collection. Blood samples were obtained immediately with retro-orbital sampling, collected in 500µL RNAprotect animal blood tubes (Qiagen, Germany), and stored at -20°C until RNA purification. Mice were then euthanized by decapitation.

2. Sample collection and microarray analysis

Total RNA was isolated from blood samples using the Rneasy Kits, a process that was automated by the QIAcube (Qiagen, Germany). RNA was cleaned, and contaminants were removed using the Rneasy MinElute CleanUp Kit (Qiagen, Germany). NanoDrop 2000 (Thermo Fisher Scientific, U.S.) and Agilent Bioanalyzer 2100 (Agilent Technologies, U.S.) were used to measure RNA yield and detect integrity before microarray analysis. Samples with an RNA integrity number (RIN) of less than 7, A260/A280 ratio of less than 1.8, and volume of less than 35uL each at 50ng/uL were excluded from the dataset (Thermo Fisher Scientific, U.S.). Reads was measured by Affymetrix Clariom S microarray (Affymetrix, Thermo Fisher Scientific).

3. Expression data analysis

All expression analysis was performed in RStudio. The limma package, which allows for variance stabilization, was used to normalize reads and identify differentially expressed genes (DEGs) across sex and age from raw data CEL files ($|\log_2 FC| \geq 1.5$, p-vale ≤ 0.05) (20). An ExpressionSet object containing expression and phenotype data was created and used in all downstream analyses. Exploratory data analysis techniques, including heatmaps, principal component analysis (PCA), and clustering, were employed to examine data. The volcano plot and heatmap for DEGs were plotted with the R packages ggplot2 and pheatmap. DEGs were exported to Cytoscape Version 3.9.1 to

visualize their interactive network. Protein-protein interaction networks (PPIs) of DEGs were constructed with STRING (https:// string-db.org). MCODE V1.5.1 was used to identify significant modules (MCODE score ≥ 4). Hub genes were selected using CytoHubba. GeneCards was used to look up previous finding and gene functions (21).

R/Bioconductor package gProfiler was used for functional enrichment analysis. gProfiler computes the enrichment of a pathway from the input gene list using Fisher's exact test and multiple-test correction (22). Cell Marker 2.0 and clusterProfiler were used to infer the cell types in which the DEGs might be found (23,24). NetworkAnalyst platform and miRTarbase were used to predict miRNA–gene interaction (25). ChIP Enrichment Analysis (ChEA) was used to obtain transcription factors (TFs). Based on experimental evidence, ChEA is specifically designed to link TFs to their target genes and link them to the DEGs (26). Additional graphs were visualized in BioRender.

4. Cross-validation

Findings were compared to previous studies from the Gene Expression Omnibus (GEO) database to validate the findings. The search query [ischemic stroke AND (reperfusion OR middle cerebral occlusion) AND peripheral blood] was used to obtain studies surveying transcriptional changes in peripheral blood post-recanalization. Datasets GSE16561 (27) and GSE21136 (28) were collected from the GEO database. GSE16561 is comprised of clinical data analyzing blood expression from patients with MRI-diagnosed ischemic stroke, including those who received rt-PA (within 3 hours from onset) and controls (27). GSE21136 includes microarray analysis on rats that received MCAO+Recan with and without rtPA (28). Similar differential gene expression and functional enrichment analyses were performed on these datasets in R. All data in this study is available in the GEO database under accession number GSE278554.

Results

Following the reading of raw CEL files and normalization with rma, the entire dataset was assigned to an ExpressionSet object, which consists of 44 samples and 29,129 quantified transcripts. A heatmap plot identified four clusters of genes, with one corresponding primarily to differences due to sex **(Figure 1A**). PCA confirmed that the SHAM and MCAO samples were closely clustered, whereas the MCAO+Recan group showed a more significant difference (**Figure 1B**). Using an exploratory approach to allow for a broader survey of potential associations or relationships in these early transcriptional changes, differential gene expression (MCAO vs. SHAM and MCAO+Recan vs. SHAM) was analyzed. DEGs with a less conservative filter ($|\log_2 FC| \geq 1.5$, $p \leq 0.05$) were identified and reported with adjusted p-values along with raw p-values (**Supplementary Table 1**).

1. Differential expression analysis

Differential gene expression analysis identified 4 significantly upregulated genes in the MCAO group compared to SHAM, *Plet1, Krt13, Psca,* and *Gsto1* ($|\log_2 FC| \geq 1.5$, $p \leq 0.05$) (**Figure 1C**; **Supplementary Table 1**). These genes have been previously associated with tumour, cancer, and tissue damage (29–32). *Plet1* is a progenitor cell marker predicted to be involved in cell-matrix adhesion, cell migration, and wound healing (30). *Krt13* is related to inflammation, tissue damage, and epithelial proliferation and differentiation (33). *Gsto1* has previously been associated with inflammatory responses (34). However, to date, these have not been associated with ischemic stroke.

MCAO+Recan saw an increased number of DEGs, with 12 significantly upregulated genes (*Il1r2, Hdc, Tarm1, Mrgpra2a, Mrgpra2b, Mt1, Mmp8, Ngp, Vcan, Lrg1, Cd14,* and *Ms4a6d*) and 7 significantly downregulated genes (*Cd55, Cd69, Pou2af1, Ly6d, H2-Oa, Ptprcap*, and *Ms4a1*) ($|\log_2 FC| \geq 1.5$, $p \leq 0.05$) (**Figure 1C**; **Supplementary Table 1**). Cross-checking with GeneCard identified *Il1r2, Hdc, Mt1, Mmp8, Ngp, Vcan, Lrg1, Cd14, Ms4a4a, Ms4a6d,* and *Cd69* as genes previously linked to ischemic stroke and immune-related pathogenesis (21). The anti-inflammatory marker *Cd55*, which has neuroprotective properties against ischemia-reperfusion injuries (35), is downregulated. Previous studies suggested that *Lrg1* is a blood biomarker that predicts neurological recovery after stroke within three months, as it is upregulated in patients suffering from cerebral ischemia but downregulated after rehabilitation. *Lrg1* also promotes apoptosis through the TGFβ-Smad1/5 signalling pathway in mice (36) and angiogenesis in ischemic rats' brains via the TGF-β1 pathway (37). *Mmp8* expression is associated with high risks of ischemia, and decreased MMP8 protein levels improve neurological functions and reduce MCAO infarct size in rats (38). *Cd69* plays a role in downregulating endothelial activation and reduces brain damage post-ischemia (39). Delivering hematopoietic stem/progenitor cells-derived *Mt1* offers neuroprotective effects after ischemia-reperfusion injury in mice (40).

Next, the roles of sex and age in transcriptional changes following ischemia were investigated. The findings indicate that young MCAO animals exhibited a greater degree of transcriptional changes, showing a higher number of DEGs compared to aged animals (**Figure 2B**). In the MCAO group, young animals had 50 DEGs, while aged animals only had 2 DEGs. Similarly, young animals displayed 90 DEGs in the MCAO+Recan condition, whereas aged mice had 22 DEGs (**Figure 2A**).

Notably, female MCAO animals had more DEGs than their male counterparts (**Figure 2B**). Female MCAO+Recan animals showed 12 DEGs, while female MCAO animals had 3 DEGs. Their male counterparts exhibited 1 DEG and 10 DEGs, respectively (**Figure 2A**).

As verified using GeneCards, these DEGs include previously inflammatory linked genes such as *Il1r2, Cd244, Il1rn, Mmp8, Ccr2, Tnfaip2, Gsto1* (young MCAO), *Ifi203* (aged MCAO), *Cxcr2, Il1f9, Ifi203, Romo1, Pdcd5, Cd33, Hsbp1, Mmp8* (young

MCAO+Recan), *Tarm1, Cxcr5, Cd79b*, and *Cd14* (aged MCAO+Recan) (21). Some of these genes, such as *Mmp8* (41), *Ccr2* (42), and *Cxcr2* (43), have previously been associated with ischemic stroke.

The female MCAO and MCAO+Recan groups shared 15 DEGs, which include *Asprv1, Cbr2, Cxcr2, Emp1, Gsto1, Hdc, Il1b, Il1rn, Lrg1, Mmp8, Mrgpra2a, Plet1, Prg4*, and *Sirpb1a*. Additionally, the female MCAO+Recan group shared the *Ly6d* and *Ptprcap* genes with their male counterparts (**Figure 2A**).

In young animals with MCAO or MCAO+Recan, there were 6 common DEGs: *Asprv1, Hdc, Il1r2, Il1rn, Mmp8,* and *Pla2g7*. However, when comparing young and aged animals in the MCAO+Recan group, the only shared gene is interleukin 1 receptor type II (*Il1r2*) (**Figure 3A**).

It is important to note that, despite the identification of 19 unique DEGs in MCAO+Recan, not all of them exhibited uniform expression trends across treatment groups, as *Cd14, Mrgpra2a, Mrgpra2b, Ly6d, Vcan,* and *Mt1* showed sex- and age-specific expression patterns (**Supplementary Figure 2**). The upregulation of *Cd14* post-recanalization was mainly driven by the aged group (**Supplementary Figure 2A**). *Mrgpra2a* and *Mrgpra2b* increased expression levels were primarily observed in female MCAO+Recan animals (**Supplementary Figure 2B-C**). The differential changes in *Ly6d, Vcan,* and *Mt1* expression levels were observed in all subgroups within MCAO+Recan except for young males (**Supplementary Figure 2D-F**).

2. Enrichment analysis

The PPI network of 19 DEGs of the MCAO+Recan group was constructed with STRING. The hub genes *Il1r2, Cd55, Mmp8, Cd14*, and *Cd69* were identified using the DMNC algorithm of the plug-in CytoHubba (**Figure 3A**). Since the number of DEGs in the MCAO group was low, the analysis for this group yielded no results.

To gain further biological and cell-specific context, the 19 DEGs from the MCAO+Recan group were assessed with gProfiler. The analysis showed that these DEGs were mainly involved in leukocyte activation (*Cd55, Tarm1, Mmp8, Pou2af1, Ly6d, H2-Oa, Ms4a1*), cytokine production (*Il1r2, Cd55, Tarm1, Mmp8, Pou2af1, Cd14*), and lymphocyte activation (*Cd55, Tarm1, Pou2af1, Ly6d, H2-Oa, Ms4a1*) (**Figure 3B**).

The GSE16561 and GSE21136 datasets, consisting of human and rat ischemic samples, were used to validate the expression of the MCAO+Recan DEGs (**Figure 3C**). *Vcan* was the only DEG found in all three datasets of recanalization: GSE1656 (humans), GSE21136 (rats), and this mouse data. This suggests that Vcan is an important and novel marker of recanalization that is highly conserved across species. *Il1r2* and *Vcan* were shared between MCAO+Recan mice and rats. *Vcan* and *Cd14* were shared between MCAO+Recan mice and human samples. Proinflammatory *Il1r2* and *Cd14* were both hub genes, suggesting they may play a critical role in reperfusion injury and early recanalization responses.

When breaking MCAO+Recan enrichment analysis down to age- and sex-specific groups, immune system process was significantly enriched in the MCAO+Recan. This included downregulated genes in female (*Cd55, Prg4, Ets1, Pou2af1, Cxcr5, Cd79b, Cd83, Blk, Ly6d, H2-Oa, Mzb1, Ms4a1*) (**Figure 5A**) and aged animals (*Cd55, Stap1, Cxcr5, Cd79b, Gpr18, Ly6d, Ms4a1*) (**Figure 6B**). The immune system process was also linked to upregulated genes in the female (*Cxcr2, Gpr35, Cd244a, Il36g, Il1rn, Lcn2, Il1b, Mafb, S100a8, Sirpb1a, Tlr2, S100a9, Csf3r, Bst1, Clec4d, Clec4e, Ifitm1, Nlrp12, Tarm1, Trim30b, Adam8, Ifitm2, Ifitm6, Hmox1, Hp, Mmp8, Ccr2, Alas1, Myd88, Ccr1, Tlr13, Trpm2, Lilrb4b, Lilrb4a, Osm, Wfdc17, Wfdc21, Cd300lf, Arg2, Olfm4, Acod1, Il1rap, Retnlg, App, Fpr2, Pla2g7, Trem1, Fpr1, Dusp1, Cd14, Slc15a3*) (**Figure 5A**), aged (*Gpr35, Mafb, Fcgr1, Tarm1, Ctsl, Acod1, Pram1, Cd14, Il1r2*) (**Figure 6B**), and young animals (*Cxcr2, Il36g, Il1rn, Lcn2, Hp, Mmp8, Rab27a, Pla2g7*) (**Figure 6A**). Many DEGs were shared between these groups, such as the downregulated *Cd55, Cxcr5, Cd79b, Ly6d, Ms4a1* and the upregulated *Cxcr2, Gpr35, Il1r2,* and *Arg2*.

Females and young MCAO+Recan also saw an enrichment in cytokine production and regulation. These pathways were driven by upregulated *Il1r2, Cxcr2, Gpr35, Chil1, Il1rn, Il1b, Tlr2, Csf3r, Ifitm1, Nlrp12, Ifitm2, Ifitm6, Ccr2, Myd88, Ccr1, Il13ra1, Osm, Wfdc21, Cd300lf, Socs3, Il1rap, App, Dusp1, Cd14, Csf2ra* in females (**Figure 5A**), and *Il1r2, Cxcr2, Il36g, Il1rn* in young animals (**Figure 6A**).

Other inflammatory pathways, such as lymphocyte activation and differentiation, were enriched in female and aged MCAO+Recan. Lymphocyte activation was driven by downregulated *Cd55, Cxcr5, Cd79b, Gpr18, Ly6d, Ms4a1* in the aged group (**Figure 6B**) and upregulated *Cd244a, Il1b, Mafb, Sirpb1a, Clec4d, Clec4e, Tarm1, Adam8, Ccr2, Myd88, Lilrb4b, Lilrb4a, Arg2* in the female group (**Figure 5A**). On the other hand, lymphocyte differentiation was observed in the female group with downregulated *Pou2af1, Cd79b, Cd83, Ly6d, H2-Oa, Ms4a1* (**Figure 5A**) and aged group (**Figure 6B**) with the same genes and an additional *Gpr18*. Mononuclear cell differentiation and migration was significantly enriched in downregulated aged MCAO+Recan (*Cd79b, Gpr18, Ly6d, Ms4a1*) (**Figure 6B**) and upregulated female MCAO+Recan (*Nlrp12, Adam8, Ccr2, Ccr1, Trpm2, Retnlg, App, Fpr2, Pla2g7, Trem1, Dusp1, Pou2af1, Cd79b, Cd83, Blk, Ly6d, H2-Oa, Ms4a1*) (**Figure 5A**). Monocellular proliferation was also found in the upregulated female MCAO+Recan (*Cd244a, Il1b, Tarm1, Ccr2, Myd88, Lilrb4b, Lilrb4a, Arg2*) (**Figure 5A**).

The Cell Marker 2.0 database was used to obtain markers for various cell types across different mouse tissues and compared them against this dataset. This approach provided valuable tissue and cell-specific context for the observed transcriptional changes. In this dataset, the marker with the highest gene count was for neutrophils, with all genes being significantly upregulated and driven by the MCAO+Recan group, with the greatest expression in female and aged mice (**Figure 6A**). This suggests that neutrophil markers were highly expressed and contributed to ischemic pathogenesis and

reperfusion injury post-recanalization. Downregulated DEGs were mostly markers of macrophages, lymphocytes, T cells, B cells, and arterial cells (**Figure 6A**).

The female MCAO+Recan also showed the highest number of enriched pathways related to neutrophil activity, such as neutrophil migration (*Cxcr2, Il1b, Bst1, Adam8, Myd880*), chemotaxis (*Cxcr2, Il1b, S100a8, S100a9, Csf3r, Bst1, Trem1*), aggregation (*Il1b, S100a8, S100a9, Adam8*), and degranulation (*Cxcr2, Chil1, Cd55, Lcn2, S100a8, Sirpb1a, S100a9, Clec4d, Tarm1, Cd33, Adam8, Mcemp1, Hp, Mmp8, Trpm2, Lilrb4b, Lilrb4a, Olfm4, Fpr2, Fpr1, Cd14*) (**Figure 6B**).

Other potential pathways that may connect to reperfusion injury and futile recanalization in this group were leukocyte activation (*Cxcr2, Cd244a, Cd55, Il1b, Mafb, Sirpb1a, Tlr2, Clec4d, Clec4e, Tarm1, Adam8, Hmox1, Mmp8, Pou2af1, Ccr2, Cxcr5, Myd88, Lilrb4b, Lilrb4a, Cd79b, Cd300lf, Arg2, Cd83, Blk, Ly6d, App, H2-Oa, Mzb1, Ms4a1), leukocyte cell-cell adhesion (Cd244a, Cd55, Il1b, S100a8, Sirpb1a, S100a9, Tarm1, Adam8, Ets1, Ccr2, Lilrb4b, Lilrb4a, Arg2, Cd83, H2-Oa, Lrg1*), and leukocyte proliferation (*Cd244a, Cd55, Il1b, Tarm1, Ccr2, Myd88, Lilrb4b, Lilrb4a, Arg2, Blk, Mzb1, Csf2ra*). In addition, significant leukocyte differentiation (*Mafb, Cd79b, Ctsl, Gpr18, Ly6d, Ms4a1*), leukocyte chemotaxis (*Gpr35, Stap1, Cxcr5, Gpr18*), and leukocyte activation (*Cd55, Mafb, Stap1, Tarm1, Cxcr5, Cd79b, Ctsl, Gpr18, Ly6d, Pram1, Ms4a1*) were found in the aged MCAO+Recan (**Figure 6B**).

The high degree of expression in neutrophil-associated pathways in these samples was then compared against other data sets related to recanalization after stroke. The female MCAO+Recan group was compared to the human female samples GSE1656 (GSE21136 was excluded as it consists of only male samples) and 37 shared orthologues, including the hub genes *Il1r2, Mmp8, Cd14*, and *Cd55* were identified (**Figure 7A**). Notably, *Vcan* was also significantly upregulated in both female mice and female patients. Furthermore, the two groups shared a considerable number of enriched pathways (**Figure 7B**), many of which were related to neutrophil and leukocyte activity (**Figure 7C**). This indicates a highly conserved pattern of post-recanalization leukocyte- and neutrophil activities across species that can be linked to reperfusion injury.

3. Regulatory network

Using NetworkAnalyst, the miRNAs that regulated DEGs in MCAO+Recan were predicted. The top regulated nodes (degree ≥ 10) were identified to be *Clec7a, Cd69, Ets1, Cxcr2, Macf1, Csf3r, Csf1, Btc, Vcan, Entpd1, Slc11a2, Cxcr2, Fitm2, Lmbrd1, Pafah1b2*, and *Gsk3b* (**Supplementary Figure 3**).

Notably, Vcan was the sole node in aged MCAO+Recan and one of the central nodes in female MCAO+Recan. It was regulated by mmu-mir-450b-5p, mmu-mir-143-3p, mmu-mir-340-5p, mmu-mir-680, mmu-mir-690, mmu-mir-185-5p, mmu-mir-203-5p, mmu-mir-129-5p, mmu-mir-3079-5p, mmu-mir-434-3p in the aged group, and the

additional mmu-mir-203-5p and mmu-mir-185-5p in female group (**Supplementary Figure 3**). Vcan was an upregulated gene involved in the cell adhesion pathway in the female group (**Figure 4A**) and in the extracellular region for both the female and aged groups (**Figure 5B**). This suggests that *Vcan* plays a role in remodeling the extracellular matrix (ECM) during neutrophil migration and adhesion in reperfusion injury.

The top 50 TFs that regulated DEGs in MCAO+Recan groups were exported from ChEA3. NFE4 and MTF1 had the highest confidence score, 9.0 and 10.0, respectively, and they regulated genes in female MCAO+Recan **(Supplementary Figure 4)**. NFE4 regulated mostly proinflammatory genes, namely *P2ry13, Ifitm2, Csf3R, Fpr1, Mcemp1, Fpr2, Csf2Ra, Trem1, Bst1, Nlrp12, Clec4D, Cxcr2, Adam8, Clec4E, Cd300Lf, Myd88, Cd33, Ccr2*, and *Tlr2*. MTF1 targeted more specific leukocyte differentiation and leukocyte aggregation and migration, including *Il1rn, Csf3R, Fpr1, Tnfaip2, Fpr2, Csf2ra, Trem1, Pla2g7, Socs3, Clec7A, Cxcr2, Upp1, Cd14, Cd300lf, Slc15A3, Slc16A3, Ier3, Ccr1, Osm, Acod1, Il36G, Cyb561A3, Fosl2, Bst1, Nlrp12, Clec4D, Mafb, Il1B, Adam8, Clec4E, S100A9, Myd88*, and *Tlr2*. These two TFs co-regulated multiple genes, namely *Cd300lf, Csf2ra, Nlrp12, Clec4d, Csf3r, Trem1, Cxcr2, Adam8, Fpr1, Fpr2,* and *Bst1*.

Among the regulated genes, 16/19 of NFE4 targeted genes (*Csf3R, Fpr1, Mcemp1, Fpr2, Csf2Ra, Trem1, Bst1, Nlrp12, Clec4d, Cxcr2, Adam8, Clec4e, Cd300lf, Myd88, Cd33, Ccr2, Tlr2*) and 17/33 of MTF1 targeted genes (*Csf3R, Fpr1, Tnfaip2, Fpr2, Csf2Ra, Trem1, Pla2G7, Socs3, Clec7A, Cxcr2, Upp1, Cd14, Cd300lf, Slc15A3, Slc16A3, Ier3, Ccr1, Osm, Acod1, Il36g, Cyb561A3, Fosl2, Bst1, Nlrp12, Clec4d, Mafb, Il1b, Adam8, Clec4e, S100A9, Myd88, Tlr2*) were implicated in neutrophil migration, degranulation, chemotaxis, and migration, both involved in neutrophil migration and degranulation (**Figure 4A**). Combining these multifaceted data, a network illustrating how DEGs, miRNAs, and TFs interact to upregulate neutrophil activity, implicating reperfusion injury, particularly in females, was constructed (**Figure 8**).

Discussion

Several blood biomarkers have already been identified with high sensitivity for stroke diagnosis, such as S100B (glial activation), vWF (thrombosis), MMP9, and VCAM (inflammation), which are used to discriminate stroke from healthy controls (44). As the number of candidate biomarkers continues to rise, they offer additional insights into clinical responses to medical interventions and outcome predictions. However, there are currently no biomarkers for the early prediction of risks of poor recovery following recanalization in ischemic stroke. The requirements for such biomarkers, including high sensitivity, specificity, and rapid turnaround time, also make their development challenging. Identifying blood biomarkers could revolutionize stroke care, enhancing prognosis and recovery with personalized treatment. At-risk patients can then benefit from early additional therapies such as neuroprotective or anti-inflammatory. Moreover,

these biomarkers could help stratify patients in clinical trials, offering better insights into the mechanisms of injury and recovery. The quest for reliable biomarkers is, therefore, critical to improving post-recanalization outcomes and reducing long-term disability in stroke survivors.

This study investigated the regulation of genes associated with recanalization by transcription factors and miRNAs, uncovering early changes driven by neutrophil activity were the potential mechanisms behind reperfusion injury and futile recanalization. In the co-regulatory network, several nodes exhibited high centrality, including five hub genes—*Il1r2, Cd55, Mmp8, Cd14, and Cd69*—along with two transcription factors, MTF1 and NFE4, and multiple miRNAs. These regulatory elements were predominantly associated with neutrophil activity, offering a deeper understanding of gene regulatory mechanisms involved in reperfusion injury and recovery post-recanalization.

Upon further analysis of the hub genes, *Il1r2* expression may play a regulatory role in modulating the inflammatory response by reducing IL-1 activity, potentially influencing stroke outcomes by limiting excessive inflammation (45). *Cd55* can protect brain tissue in ischemic stroke by inhibiting the complement system, preventing excessive inflammation and complement-mediated damage to neurons, glial cells, and the blood-brain barrier. This regulation helps preserve tissue integrity and reduce secondary injury following the initial ischemic event (35). *Mmp8*, primarily produced by neutrophils, facilitates neutrophil migration and plays a role in degrading the ECM components, thereby modulating inflammation. In ischemic stroke, *Mmp8* may contribute to the breakdown of the blood-brain barrier and tissue remodeling (41). Additionally, *Cd69* and *Cd14* are integral components of the core inflammatory program governing neutrophil activity during ischemic stroke. For instance, *Cd69* dampens endothelial activation during ischemic events, and its deficiency in mouse models is linked to increased neutrophil infiltration and larger infarct volumes (39). *Cd14*, on the other hand, triggers neutrophil responses through toll-like receptors, amplifying the inflammatory response. Elevated *Cd14* expression has been associated with worse stroke outcomes due to increased inflammation (46). However, a limitation of this study lies in distinguishing whether these transcriptional changes were driven by reperfusion injury following recanalization or the length of the recovery period post-stroke onset.

miRNAs, which directly influence mRNA expression, also play a crucial role in this regulatory network. The most connected genes in this miRNA analyses were *Clec7a, Cd69, Ets1, Cxcr2, Macf1, Csf3r, Csf1, Btc, Vcan, Entpd1, Slc11a2, Cxcr2, Fitm2, Lmbrd1, Pafah1b2*, and *Gsk3b*. The genes *Cxcr2, Vcan, Gsk3b, Csf3r*, and *Ets1* were particularly relevant to neutrophil migration and ECM remodeling, the critical processes of ischemic stroke. For instance, CXCR2 is a chemokine receptor critical for neutrophil migration. It binds to chemokines like CXCL1 and CXCL8, directing neutrophils to sites of inflammation during ischemic stroke. CXCR2 has a direct role in recruiting neutrophils to damaged brain tissue, contributing to inflammation and stroke pathology

(13). CSF3R is the receptor for granulocyte colony-stimulating factor, which regulates neutrophil production and release (47). The roles of some other genes are less clear. GSK3B is a kinase involved in cell migration, proliferation, and apoptosis. It also regulates ECM components and may be involved in stroke recovery by modulating tissue remodelling (48). MACF1 is involved in cytoskeleton dynamics, essential for cell migration and structural integrity (49). Though its direct role in ischemic stroke is unclear, MACF1 could affect cell migration, including neutrophil motility and tissue repair processes.

The functional enrichment analysis here highlighted that the biological processes regulated by these genes were primarily related to leukocyte and neutrophil activity. Neutrophil microcirculatory stalls represent an emerging area of research in ischemic stroke and futile recanalization. While some in-vivo imaging studies have shown neutrophil stalls in the microvasculature are the driving cause of microcirculatory failure, much remains to be learned (13).

After stroke, neutrophils heavily rely on the ECM to migrate, extravasate, and aggregate in small capillaries. Ischemic injury triggers inflammatory cytokines and chemokines, upregulating ICAM-1 and VCAM-1 on endothelial cells. Neutrophils bind to these adhesion molecules via integrins (e.g., α2β1, α4β1), and secrete MMP-9, degrading ECM components like collagen and fibronectin, facilitating extravasation. Once inside the brain parenchyma, neutrophils follow chemokine gradients (e.g., CXCL1) to migrate, but as they accumulate, they release neutrophil extracellular traps that trap more neutrophils and platelets, leading to microvascular plugging and obstruction, particularly in small vessels within the ischemic core and penumbra. The interaction between neutrophils and the altered ECM thus plays a crucial role in their ability to migrate and aggregate after a stroke, causing reperfusion injury and potential futile recanalization.

Vcan, encoding the large extracellular matrix chondroitin sulfate proteoglycan versican, emerged from this study as a novel player in ECM-driven neutrophil-mediated microcirculatory failure or reperfusion injury. Interestingly, *Vcan* has not been previously investigated in the context of ischemic stroke or futile recanalization, despite this study's observation of its significantly conserved increased expression across species that underwent recanalization treatment. In traumatic brain injury, it was shown that FOXO1 protein is induced in neutrophils after injury, and FOXO1 upregulates cytoplasmic Vcan. These FOXO1-high neutrophils infiltrate the brain, promoting the aggregation and activation of other immune cells, exacerbating brain damage (50). In other pathologies, during the recovery phase, *Vcan* and other ECM proteoglycans play a crucial role in ECM remodelling, interacting with proteins and molecules to maintain ECM structure and stability. *Vcan* not only acts as a biomarker of peripheral ECM remodelling but also serves as a repository for cytokines that regulate immune cell behavior (51). These dynamic interactions between ECM and neutrophils, where neutrophils contribute to

ECM remodelling via enzymes like neutrophil elastase and matrix metalloproteinases, while the ECM influences neutrophil function, highlight the bidirectional relationship that drives inflammation and recovery. *Vcan*'s role in this process emphasizes its significance in shaping the inflammatory microenvironment, influencing both neutrophil activity and ECM integrity, which are vital to stroke progression and post-reperfusion outcomes. Beyond these connections, however, little is known regarding *Vcan*'s role in stroke or recanalization outcomes, marking it as an intriguing target for further research.

In aged animals, *Vcan* was significantly regulated by mmu-mir-450b-5p, mmu-mir-143-3p, mmu-mir-340-5p, mmu-mir-680, mmu-mir-690, mmu-mir-185-5p, mmu-mir-203-5p, mmu-mir-129-5p, mmu-mir-3079-5p, mmu-mir-434-3p, and the additional mmu-mir-203-5p and mmu-mir-185-5p for female MCAO+Recan. Some of these miRNAs already have established roles in ischemic stroke. miR-143-3p and miR-185-5p are highly sensitive markers of ischemic stroke in clinical patients (52,53). miR-143-3p plays a role in vascular remodelling, integrity, and angiogenesis by regulating vascular smooth muscle cells, which are crucial for stroke recovery and reperfusion (52). Meanwhile, miR-185-5p demonstrates neuroprotective effects in ischemic stroke by targeting genes involved in oxidative stress and apoptosis. Overexpression of miR-185-5p has been shown to protect neurons from ischemic injury by inhibiting pro-apoptotic genes like Caspase-3 and reducing oxidative stress through the NF-κB pathway (53).

Additionally, miR-450b-5p is highly expressed in thrombi retrieved via EVT from stroke patients (54), while miR-340-5p exhibits anti-inflammatory properties, inhibiting pro-inflammatory cytokines such as TNF-α and IL-1β. Overexpression of miR-340-5p in stroke models reduces infarct size and improves functional recovery by mitigating inflammation (55). miR-129-5p further enhances ischemic brain recovery by binding to SIAH1 and activating the mTOR signalling pathway, preventing neuronal apoptosis (56). Together, these findings suggest that these miRNAs, specifically those found to be modulating Vcan, represent potential therapeutic targets, offering promising avenues for future interventions to improve clinical outcomes following recanalization.

The data here showed that NFE4 are MTF1 were the TFs with the highest scores in the entire dataset, regulating 19 and 33 genes, respectively, in the female MCAO+Recan group. Among these, 16/19 and 17/33 were implicated in neutrophil migration, degranulation, chemotaxis, and migration. The high number of genes linked to neutrophil function suggests that NFE4 and MTF1 were central regulators in mediating the recruitment and activity of neutrophils, which could profoundly affect stroke recovery and outcomes, positioning them as key players in the reperfusion injury after ischemic stroke. Previous studies demonstrated that in brain ischemia induced by transient middle cerebral occlusion, MTF-1 was triggered by a subsequent temporary femoral artery occlusion, mediating neuroprotective mechanisms against oxidative and hypoxic stress. MTF-1 also translocate to the nucleus and induces NCX1 upregulation, which has been

demonstrated to be neuroprotective (57). NFE4, however, has not been linked to stroke before.

TFs function as regulators that modulate transcriptional output, thereby controlling cell fate decisions and inflammatory responses. Previous studies showed that TFs instruct a transcriptional program that allows the developmental transition from neutrophil precursors into mature neutrophils (58). However, the molecular mechanisms underlying neutrophil differentiation and function during inflammation remain largely uncharacterized. By regulating genes involved in neutrophil migration, degranulation, chemotaxis, and cellular migration, NFE4 and MTF1 likely influence the timing, intensity, and localization of neutrophil activity in the ischemic brain. For instance, genes under their control could dictate how quickly neutrophils are recruited to the injury site, the extent to which they degranulate to release enzymes that break down damaged tissue, and how they move through the damaged brain microenvironment. Such regulation is critical because an excessive or prolonged neutrophil response can lead to blood-brain barrier disruption, increased infarct size, and further neuronal death.

In contrast, a finely tuned response can promote tissue repair and resolution of inflammation. Thus, the role of NFE4 and MTF1 in modulating neutrophil-related genes highlights their importance in balancing these opposing outcomes. On one hand, they facilitate necessary immune functions that clear damaged cells and initiate healing, while on the other, they must restrain excessive inflammation to prevent further injury. The ability of these transcription factors to tightly regulate neutrophil behaviour may be critical in determining whether stroke recovery proceeds in a neuroprotective or detrimental direction, influencing both short-term recovery and long-term neurological outcomes. Understanding the precise mechanisms by which NFE4 and MTF1 control these processes could open avenues for developing targeted therapies that modulate neutrophil responses, potentially minimizing damage and enhancing recovery in stroke patients.

Conclusion

This study shed light on the critical role of gene regulatory networks in the pathophysiology of ischemic stroke, particularly in early recanalization responses. By identifying essential hub genes—*Il1r2, Cd55, Mmp8, Cd14,* and *Cd69*—and the novel marker *Vcan*, this study uncovered genomic indicators of recanalization that are highly conserved across species, from mice to humans. *Vcan* presents a promising target for future investigation, as its interaction with neutrophils during microcirculatory stalls and high degree of conservation across species may offer new therapeutic avenues. The functional enrichment analysis also revealed that pathways related to leukocyte migration, neutrophil activation, and phagocytosis were enriched in female mice and conserved in human recanalization models, pointing to potential sex-specific differences in reperfusion injury and stroke recovery mechanisms. The discovery of transcription

factors NFE4 and MTF1, alongside miRNAs involved in reperfusion and recanalization injury, provides deeper insight into the regulatory dynamics of post-stroke recovery. These findings underscore the importance of targeting these molecular interactions in future therapeutic strategies. Experimental validation of these associations is essential, as it will advance understanding of stroke pathogenesis and potentially lead to novel, more effective treatments for ischemic stroke. By focusing on these molecular mechanisms, future research may enhance the efficacy of recanalization therapies, minimize futile recanalization, and ultimately improve patient outcomes in stroke recovery.

Acknowledgement

The authors thank Sima Abbasi Habashi and Patricia Kent for their continual support.

Sources of funding

This project is funded by the Canadian Institutes of Health Research (CIHR).

References

1. Brauer M, Roth GA, Aravkin AY, Zheng P, Abate KH, Abate YH, et al. Global burden and strength of evidence for 88 risk factors in 204 countries and 811 subnational locations, 1990–2021: a systematic analysis for the Global Burden of Disease Study 2021. The Lancet. 2024 May 18;403(10440):2162–203.
2. Benjamin EJ, Blaha MJ, Chiuve SE, Cushman M, Das SR, Deo R, et al. Heart Disease and Stroke Statistics-2017 Update: A Report From the American Heart Association. Circulation. 2017 Mar 7;135(10):e146–603.
3. Vaduganathan M, Mensah GA, Turco JV, Fuster V, Roth GA. The Global Burden of Cardiovascular Diseases and Risk. J Am Coll Cardiol. 2022 Dec 20;80(25):2361–71.
4. GBD 2019 Stroke Collaborators. Global, regional, and national burden of stroke and its risk factors, 1990-2019: a systematic analysis for the Global Burden of Disease Study 2019. Lancet Neurol. 2021 Oct;20(10):795–820.
5. Madsen TE, Khoury JC, Leppert M, Alwell K, Moomaw CJ, Sucharew H, et al. Temporal Trends in Stroke Incidence Over Time by Sex and Age in the GCNKSS. Stroke. 2020 Apr;51(4):1070–6.
6. Leppert MH, Burke JF, Lisabeth LD, Madsen TE, Kleindorfer DO, Sillau S, et al. Systematic Review of Sex Differences in Ischemic Strokes Among Young Adults: Are Young Women Disproportionately at Risk? Stroke. 2022 Feb;53(2):319–27.
7. Petrea RE, Beiser AS, Seshadri S, Kelly-Hayes M, Kase CS, Wolf PA. Gender Differences in Stroke Incidence and Poststroke Disability in the Framingham Heart Study. Stroke. 2009 Apr;40(4):1032–7.
8. Kanasi E, Ayilavarapu S, Jones J. The aging population: demographics and the biology of aging. Periodontol 2000. 2016 Oct;72(1):13–8.
9. Roth JM. Recombinant tissue plasminogen activator for the treatment of acute ischemic stroke. Proc Bayl Univ Med Cent. 2011 Jul;24(3):257–9.
10. Bhatia K, Bhagavan S, Bains N, French B, Siddiq F, Gomez CR, et al. Current Endovascular Treatment of Acute Ischemic Stroke. Mo Med. 2020;117(5):480–9.
11. Pham M, Bendszus M. Facing Time in Ischemic Stroke: An Alternative

Hypothesis for Collateral Failure. Clin Neuroradiol. 2016 Jun;26(2):141–51.
12. Dalkara T, Arsava EM. Can restoring incomplete microcirculatory reperfusion improve stroke outcome after thrombolysis? J Cereb Blood Flow Metab Off J Int Soc Cereb Blood Flow Metab. 2012 Dec;32(12):2091–9.
13. Bui TA, Jickling GC, Winship IR. Neutrophil dynamics and inflammaging in acute ischemic stroke: A transcriptomic review. Front Aging Neurosci. 2022;14:1041333.
14. Cowled P, Fitridge R. Pathophysiology of Reperfusion Injury. In: Fitridge R, Thompson M, Fitridge R, Thompson M, editors. Mechanisms of Vascular Disease: A Reference Book for Vascular Specialists [Internet]. Adelaide (AU); 2011 [cited 2022 Jun 29]. Available from: http://www.ncbi.nlm.nih.gov/books/NBK534267/
15. Goyal M, Menon BK, van Zwam WH, Dippel DWJ, Mitchell PJ, Demchuk AM, et al. Endovascular thrombectomy after large-vessel ischaemic stroke: a meta-analysis of individual patient data from five randomised trials. Lancet Lond Engl. 2016 Apr 23;387(10029):1723–31.
16. Shen H, Killingsworth MC, Bhaskar SMM. Comprehensive Meta-Analysis of Futile Recanalization in Acute Ischemic Stroke Patients Undergoing Endovascular Thrombectomy: Prevalence, Factors, and Clinical Outcomes. Life. 2023 Sep 26;13(10):1965.
17. El Amki M, Glück C, Binder N, Middleham W, Wyss MT, Weiss T, et al. Neutrophils Obstructing Brain Capillaries Are a Major Cause of No-Reflow in Ischemic Stroke. Cell Rep. 2020 Oct 13;33(2):108260.
18. Jickling GC, Liu D, Ander BP, Stamova B, Zhan X, Sharp FR. Targeting neutrophils in ischemic stroke: translational insights from experimental studies. J Cereb Blood Flow Metab. 2015 Jun;35(6):888–901.
19. Tang Y, Xu H, Du XL, Lit L, Walker W, Lu A, et al. Gene Expression in Blood Changes Rapidly in Neutrophils and Monocytes after Ischemic Stroke in Humans: A Microarray Study. J Cereb Blood Flow Metab. 2006 Aug;26(8):1089–102.
20. Ritchie ME, Phipson B, Wu D, Hu Y, Law CW, Shi W, et al. limma powers differential expression analyses for RNA-sequencing and microarray studies. Nucleic Acids Res. 2015 Apr 20;43(7):e47.
21. Stelzer G, Rosen N, Plaschkes I, Zimmerman S, Twik M, Fishilevich S, et al. The GeneCards Suite: From Gene Data Mining to Disease Genome Sequence Analyses. Curr Protoc Bioinforma. 2016 Jun 20;54:1.30.1-1.30.33.
22. Raudvere U, Kolberg L, Kuzmin I, Arak T, Adler P, Peterson H, et al. g:Profiler: a web server for functional enrichment analysis and conversions of gene lists (2019 update). Nucleic Acids Res. 2019 Jul 2;47(W1):W191–8.
23. Wu T, Hu E, Xu S, Chen M, Guo P, Dai Z, et al. clusterProfiler 4.0: A universal enrichment tool for interpreting omics data. Innov Camb Mass. 2021 Aug 28;2(3):100141.
24. Hu C, Li T, Xu Y, Zhang X, Li F, Bai J, et al. CellMarker 2.0: an updated database of manually curated cell markers in human/mouse and web tools based on scRNA-seq data. Nucleic Acids Res. 2023 Jan 6;51(D1):D870–6.
25. Zhou G, Soufan O, Ewald J, Hancock REW, Basu N, Xia J. NetworkAnalyst 3.0: a visual analytics platform for comprehensive gene expression profiling and meta-analysis. Nucleic Acids Res. 2019 Jul 2;47(W1):W234–41.
26. Lachmann A, Xu H, Krishnan J, Berger SI, Mazloom AR, Ma'ayan A. ChEA:

transcription factor regulation inferred from integrating genome-wide ChIP-X experiments. Bioinformatics. 2010 Oct 1;26(19):2438–44.
27. Barr TL, Conley Y, Ding J, Dillman A, Warach S, Singleton A, et al. Genomic biomarkers and cellular pathways of ischemic stroke by RNA gene expression profiling. Neurology. 2010 Sep 14;75(11):1009–14.
28. Jickling GC, Zhan X, Ander BP, Turner RJ, Stamova B, Xu H, et al. Genome response to tissue plasminogen activator in experimental ischemic stroke. BMC Genomics. 2010 Apr 21;11:254.
29. Uotani T, Sugimoto M, Ichikawa H, Tanaka S, Nagashima H, Uchida T, et al. Prostate stem cell antigen gene TT genotype and development of intestinal metaplasia in Helicobacter pylori infection. J Dig Dis. 2016 Jan;17(1):20–7.
30. Zepp JA, Zhao J, Liu C, Bulek K, Wu L, Chen X, et al. IL-17A-Induced PLET1 Expression Contributes to Tissue Repair and Colon Tumorigenesis. J Immunol Baltim Md 1950. 2017 Dec 1;199(11):3849–57.
31. Menon D, Innes A, Oakley AJ, Dahlstrom JE, Jensen LM, Brüstle A, et al. GSTO1-1 plays a pro-inflammatory role in models of inflammation, colitis and obesity. Sci Rep. 2017 Dec 19;7:17832.
32. Lian F, Xing X, Yuan G, Schäfer C, Rauser S, Walch A, et al. Farnesoid X receptor protects human and murine gastric epithelial cells against inflammation-induced damage. Biochem J. 2011 Sep 1;438(2):315–23.
33. Park EJ, Choi K, Park K. Induction of inflammatory responses and gene expression by intratracheal instillation of silver nanoparticles in mice. Arch Pharm Res. 2011 Feb;34(2):299–307.
34. Peddareddygari LR, Dutra AV, Levenstien MA, Sen S, Grewal RP. An analysis of methylenetetrahydrofolate reductase and glutathione S-transferase omega-1 genes as modifiers of the cerebral response to ischemia. BMC Neurol. 2009 Jul 22;9:37.
35. VanLandingham JW, Cekic M, Cutler S, Hoffman SW, Stein DG. Neurosteroids reduce inflammation after TBI through CD55 induction. Neurosci Lett. 2007 Sep 25;425(2):94–8.
36. Jin J, Sun H, Liu D, Wang H, Liu Q, Chen H, et al. LRG1 Promotes Apoptosis and Autophagy through the TGFβ-smad1/5 Signaling Pathway to Exacerbate Ischemia/Reperfusion Injury. Neuroscience. 2019 Aug 10;413:123–34.
37. Meng H, Song Y, Zhu J, Liu Q, Lu P, Ye N, et al. LRG1 promotes angiogenesis through upregulating the TGF-β1 pathway in ischemic rat brain. Mol Med Rep. 2016 Dec;14(6):5535–43.
38. Bai Y, Du Y, Yang Y, Wälchli T, Constanthin PE, Li F. Ultrasound-Targeted Microbubble Destruction Increases BBB Permeability and Promotes Stem Cell-Induced Regeneration of Stroke by Downregulating MMP8. Cell Transplant. 2024;33:9636897231223293.
39. Brait VH, Miró-Mur F, Pérez-de-Puig I, Notario L, Hurtado B, Pedragosa J, et al. CD69 Plays a Beneficial Role in Ischemic Stroke by Dampening Endothelial Activation. Circ Res. 2019 Jan 18;124(2):279–91.
40. Smith HK, Omura S, Vital SA, Becker F, Senchenkova EY, Kaur G, et al. Metallothionein I as a direct link between therapeutic hematopoietic stem/progenitor cells and cerebral protection in stroke. FASEB J. 2018 May;32(5):2381–94.
41. Palm F, Pussinen PJ, Safer A, Tervahartiala T, Sorsa T, Urbanek C, et al. Serum

matrix metalloproteinase-8, tissue inhibitor of metalloproteinase and myeloperoxidase in ischemic stroke. Atherosclerosis. 2018 Apr;271:9–14.
42. Fang W, Zhai X, Han D, Xiong X, Wang T, Zeng X, et al. CCR2-dependent monocytes/macrophages exacerbate acute brain injury but promote functional recovery after ischemic stroke in mice. Theranostics. 2018 Jun 6;8(13):3530–43.
43. Luo X. CXCR2 antagonism attenuates neuroinflammation after subarachnoid hemorrhage. J Stroke Cerebrovasc Dis. 2023 Sep 1;32(9):107266.
44. Jickling GC, Sharp FR. Blood biomarkers of ischemic stroke. Neurother J Am Soc Exp Neurother. 2011 Jul;8(3):349–60.
45. Boraschi D, Italiani P, Weil S, Martin MU. The family of the interleukin-1 receptors. Immunol Rev. 2018;281(1):197–232.
46. Zhou M, Wang CM, Yang WL, Wang P. Microglial CD14 activated by iNOS contributes to neuroinflammation in cerebral ischemia. Brain Res. 2013 Apr 19;1506:105–14.
47. Liu Y, Song R, Lu Z, Zhao L, Zhan X, Li Y, et al. The RNA m6A demethylase ALKBH5 drives emergency granulopoiesis and neutrophil mobilization by upregulating G-CSFR expression. Cell Mol Immunol. 2024 Jan;21(1):6–18.
48. Hajka D, Budziak B, Pietras Ł, Duda P, McCubrey JA, Gizak A. GSK3 as a Regulator of Cytoskeleton Architecture: Consequences for Health and Disease. Cells. 2021 Aug 14;10(8):2092.
49. Cusseddu R, Robert A, Côté JF. Strength Through Unity: The Power of the Mega-Scaffold MACF1. Front Cell Dev Biol. 2021 Mar 18;9:641727.
50. Zhou M, Liu YWY, He YH, Zhang JY, Guo H, Wang H, et al. FOXO1 reshapes neutrophils to aggravate acute brain damage and promote late depression after traumatic brain injury. Mil Med Res. 2024 Mar 31;11(1):20.
51. Islam S, Watanabe H. Versican: A Dynamic Regulator of the Extracellular Matrix. J Histochem Cytochem. 2020 Sep 10;68(11):763.
52. Tiedt S, Prestel M, Malik R, Schieferdecker N, Duering M, Kautzky V, et al. RNA-Seq Identifies Circulating miR-125a-5p, miR-125b-5p, and miR-143-3p as Potential Biomarkers for Acute Ischemic Stroke. Circ Res. 2017 Sep 29;121(8):970–80.
53. Wang Y, Su X, Leung GHD, Ren B, Zhang Q, Xiong Z, et al. Circulating microRNAs as diagnostic biomarkers for ischemic stroke: evidence from comprehensive analysis and real-world validation. Int J Med Sci. 2023 Jun 4;20(8):1009.
54. Kim JM, Byun JS, Kim J, Park MS, Hong SA, Nam TK, et al. Analysis of microRNA signatures in ischemic stroke thrombus. J Neurointerventional Surg. 2022 May;14(5):neurintsurg-2021-017597.
55. Zheng Y, Zhao P, Lian Y, Li S, Chen Y, Li L. MiR-340-5p alleviates oxygen-glucose deprivation/reoxygenation-induced neuronal injury via PI3K/Akt activation by targeting PDCD4. Neurochem Int. 2020 Mar 1;134:104650.
56. Lei Y, Jin X, Sun M, Ji Z. miR-129-5p Ameliorates Ischemic Brain Injury by Binding to SIAH1 and Activating the mTOR Signaling Pathway. J Mol Neurosci. 2021 Sep 1;71(9):1761–71.
57. Valsecchi V, Laudati G, Cuomo O, Sirabella R, Del Prete A, Annunziato L, et al. The hypoxia sensitive metal transcription factor MTF-1 activates NCX1 brain promoter and participates in remote postconditioning neuroprotection in stroke. Cell Death Dis. 2021 Apr 30;12(5):423.

58. Ai Z, Udalova IA. Transcriptional regulation of neutrophil differentiation and function during inflammation. J Leukoc Biol. 2020 Mar;107(3):419–30.

Figures

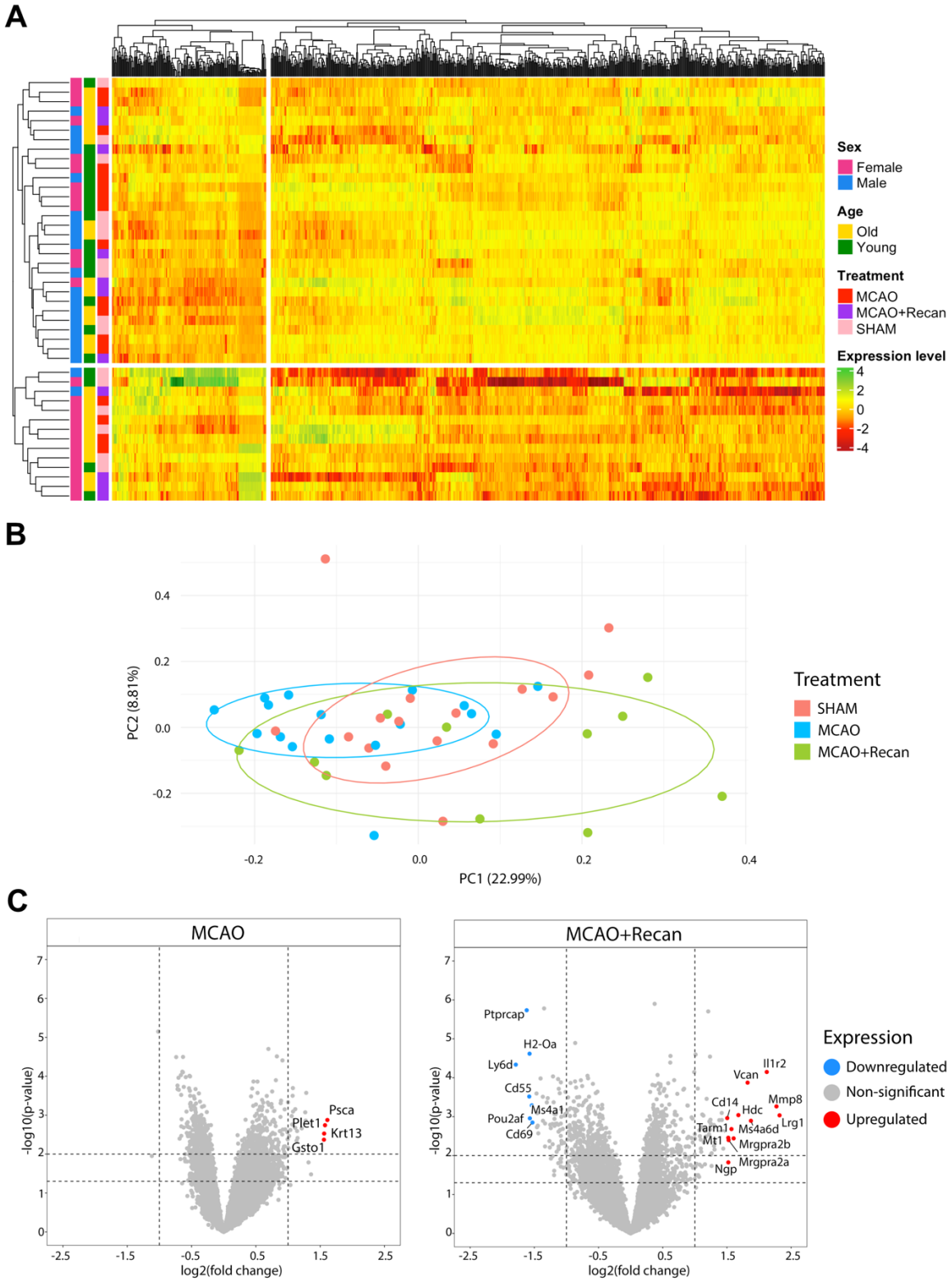

Figure 1 (A) Hierarchical clustering of gene expression patterns across all samples. The cluster dendrograms represent Canberra distance-based hierarchical clustering, which organizes samples (columns) and genes (rows) based on similarities in their expression. The dendrograms on the left and top of the heatmap display the clustering structure, visually grouping samples and genes with similar expression profiles. **(B)** Principal component analysis (PCA) of 44 samples. The PCA plot illustrates the expression variability among the samples, with each point representing the combined expression of all differentially expressed genes (DEGs) for a given sample. Samples are grouped by experimental condition (SHAM, MCAO, and MCAO+Recan), as indicated by the coloured ellipses. The x-axis represents the first principal component, which explains 22.99% of the total variance, while the y-axis represents the second principal component, explaining 8.81% of the variance. **(C)** Volcano plots of DEGs in MCAO and MCAO+Recan group. The plots depict the significantly upregulated (red) and downregulated (blue) genes in the MCAO (left) and MCAO+Recan (right) groups ($|\log2FC| \geq 1.5$, p-value ≤ 0.05). The plots compare the magnitude and significance of gene expression changes. Differential gene expression analysis was performed using the limma package in RStudio and Bioconductor.

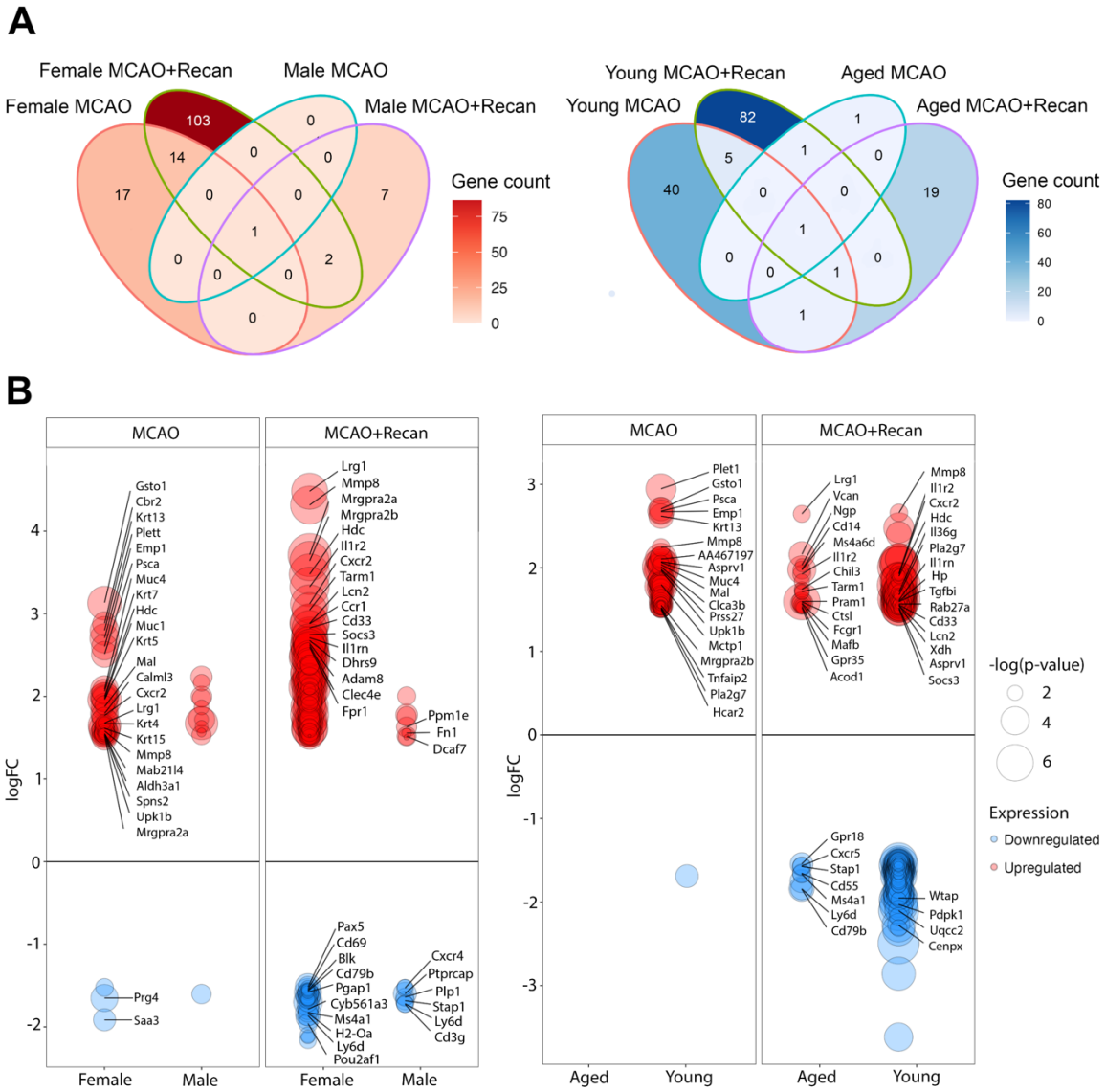

Figure 2. Age- and sex-specific differentially expressed genes (DEGs). Differential gene expression analysis was performed using the limma package from RStudio and Bioconductor. **(A)** Venn diagram showing the overlap of DEGs between sex-specific and age-specific groups (|log2FC| ≥ 1.5, p-value ≤ 0.05). **(B)** Bar plots depict the up and downregulated genes in age-specific and sex-specific groups (|log2FC| ≥ 1.5, p-value ≤ 0.05). These analyses highlight the unique and shared transcriptional changes based on age and sex in MCAO+Recan models.

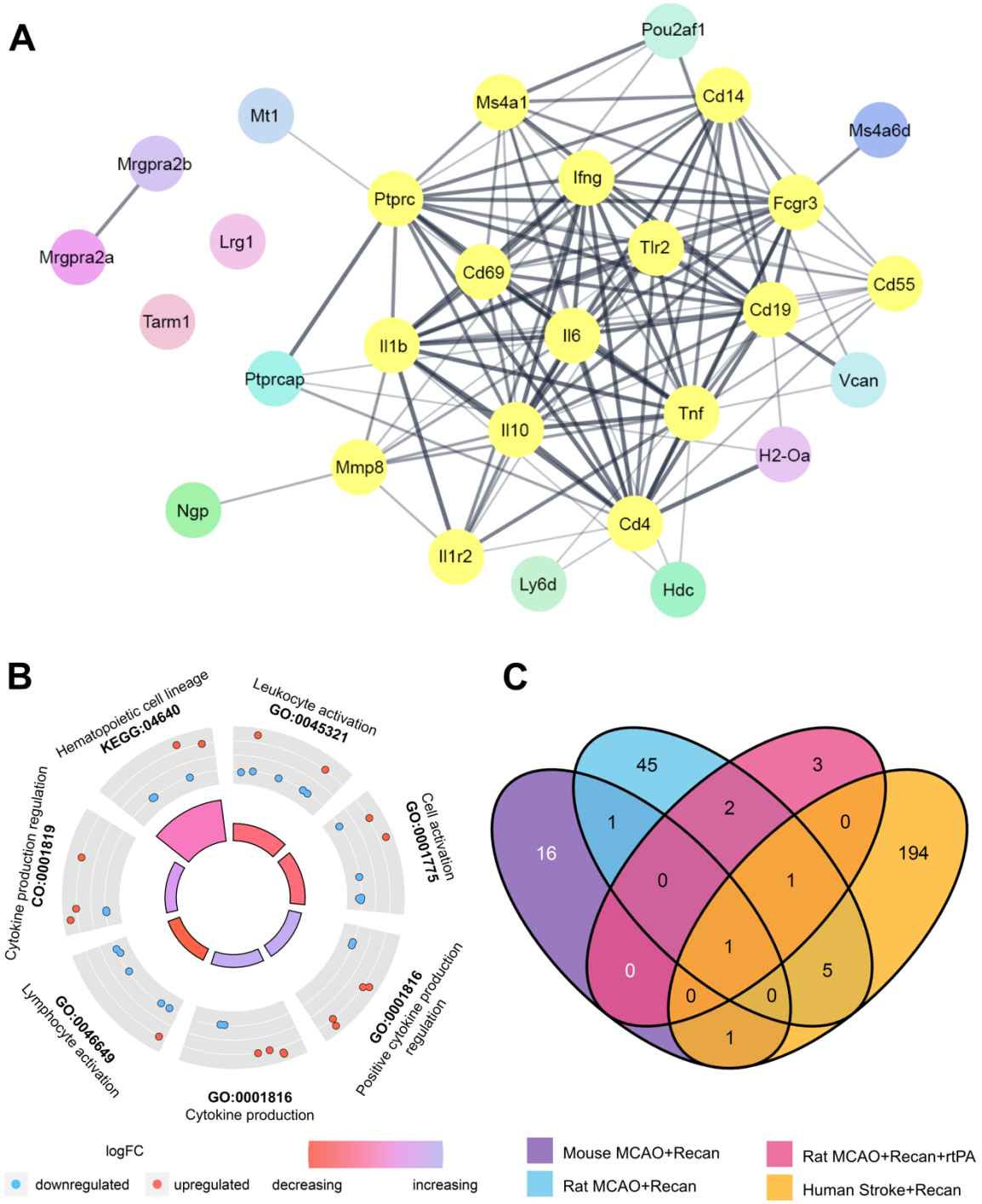

Figure 3 (A) STRING protein-protein interaction (PPI) network of differentially expressed genes (DEGs). The network was generated with a confidence level of 0.4 and a maximum of 10 additional interactors. Nodes represent DEGs, while edges indicate their interactions. Hub genes identified by the DMNC algorithm within the CytoHubba plugin are highlighted. **(B)** Circular visualization of gene annotation enrichment analysis results (GOCircle) for MCAO+Recan. Differentially expressed genes were selected (|log2FC| ≥

1.5, p-value ≤ 0.05). The inner ring features a bar plot, where bar color corresponds to the z-score (green for downregulation and yellow for upregulation), and the height of each bar represents the significance of the pathway based on log(adj p-value). The outer ring displays scatter plots of gene expression levels (logFC) for each term, with blue indicating downregulation and red indicating upregulation. **(C)** Cross-validation of all DEGs across three datasets. The analysis included mouse, GSE2113 rat samples, and GSE1656 human samples, focusing on DEGs meeting the criteria (|log2FC| ≥ 1.5, p-value ≤ 0.05). This comparison underscores the consistency of DEGs across different species and datasets.

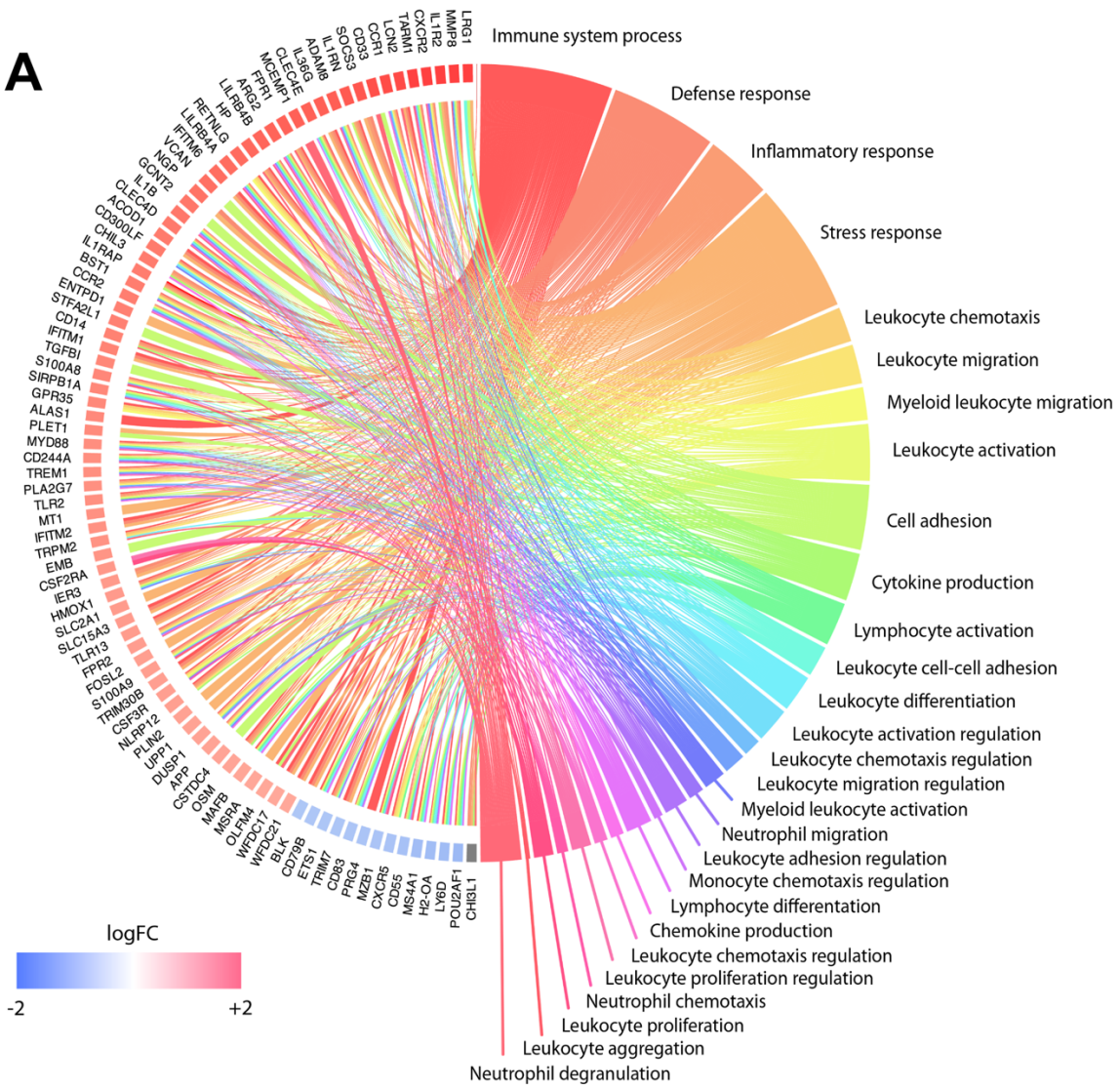
A
Immune system process
Defense response
Inflammatory response
Stress response
Leukocyte chemotaxis
Leukocyte migration
Myeloid leukocyte migration
Leukocyte activation
Cell adhesion
Cytokine production
Lymphocyte activation
Leukocyte cell-cell adhesion
Leukocyte differentiation
Leukocyte activation regulation
Leukocyte chemotaxis regulation
Leukocyte migration regulation
Myeloid leukocyte activation
Neutrophil migration
Leukocyte adhesion regulation
Monocyte chemotaxis regulation
Lymphocyte differentation
Chemokine production
Leukocyte chemotaxis regulation
Leukocyte proliferation regulation
Neutrophil chemotaxis
Leukocyte proliferation
Leukocyte aggregation
Neutrophil degranulation
LRG1
MMP8
IL1R2
CXCR2
TARM1
LCN2
CCR1
CD33
SOCS3
IL1RN
ADAM8
IL36G
CLEC4E
MCEMP1
FPR1
ARG2
LILRB4B
HP
RETNLG
LILRB4A
IFITM6
VCAN
NGP
GCNT2
IL1B
CLEC4D
ACOD1
CD300LF
CHIL3
IL1RAP
BST1
CCR2
ENTPD1
STFA2L1
CD14
IFITM1
TGFBI
S100A8
SIRPB1A
GPR35
ALAS1
PLET1
MYD88
CD244A
TREM1
PLA2G7
TLR2
MT1
IFITM2
TRPM2
EMB
CSF2RA
IER3
HMOX1
SLC2A1
SLC15A3
TLR13
FPR2
FOSL2
S100A9
TRIM30B
CSF3R
NLRP12
PLIN2
UPP1
DUSP1
APP
CSTDC4
OSM
MAFB
MSRA
OLFM4
WFDC17
WFDC21
BLK
CD79B
ETS1
TRIM7
CD83
PRG4
MZB1
CXCR5
CD55
MS4A1
H2-OA
LY6D
POU2AF1
CHI3L1
logFC
-2
+2

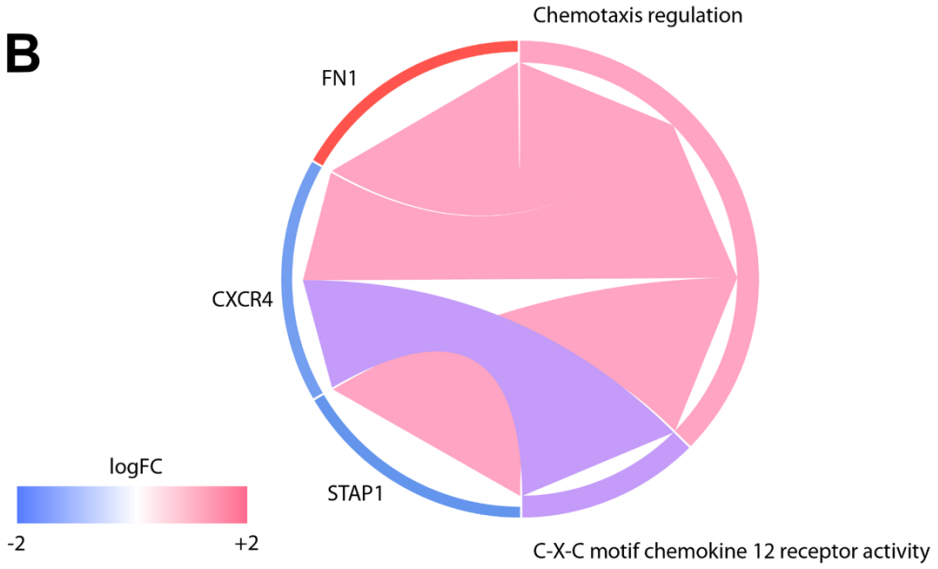
B
Chemotaxis regulation
FN1
CXCR4
STAP1
C-X-C motif chemokine 12 receptor activity
logFC
-2
+2

Figure 4. Gene ontology chord diagram illustrating core genes of significant pathways in **(A)** female and **(B)** male MCAO+Recan mice. Significant pathways are displayed on the right, while core genes are shown on the left, with their log fold change (logFC) represented by colored squares. Connections from left to right indicate gene membership within a pathway's leading-edge subset. The gost() function was employed to analyze gene ontology using gene identifiers from the differential expression results. The analysis was conducted for Mus musculus, with parameters set to evcodes=TRUE and significant=TRUE (p-value ≤ 0.05) to highlight relevant pathways and genes.

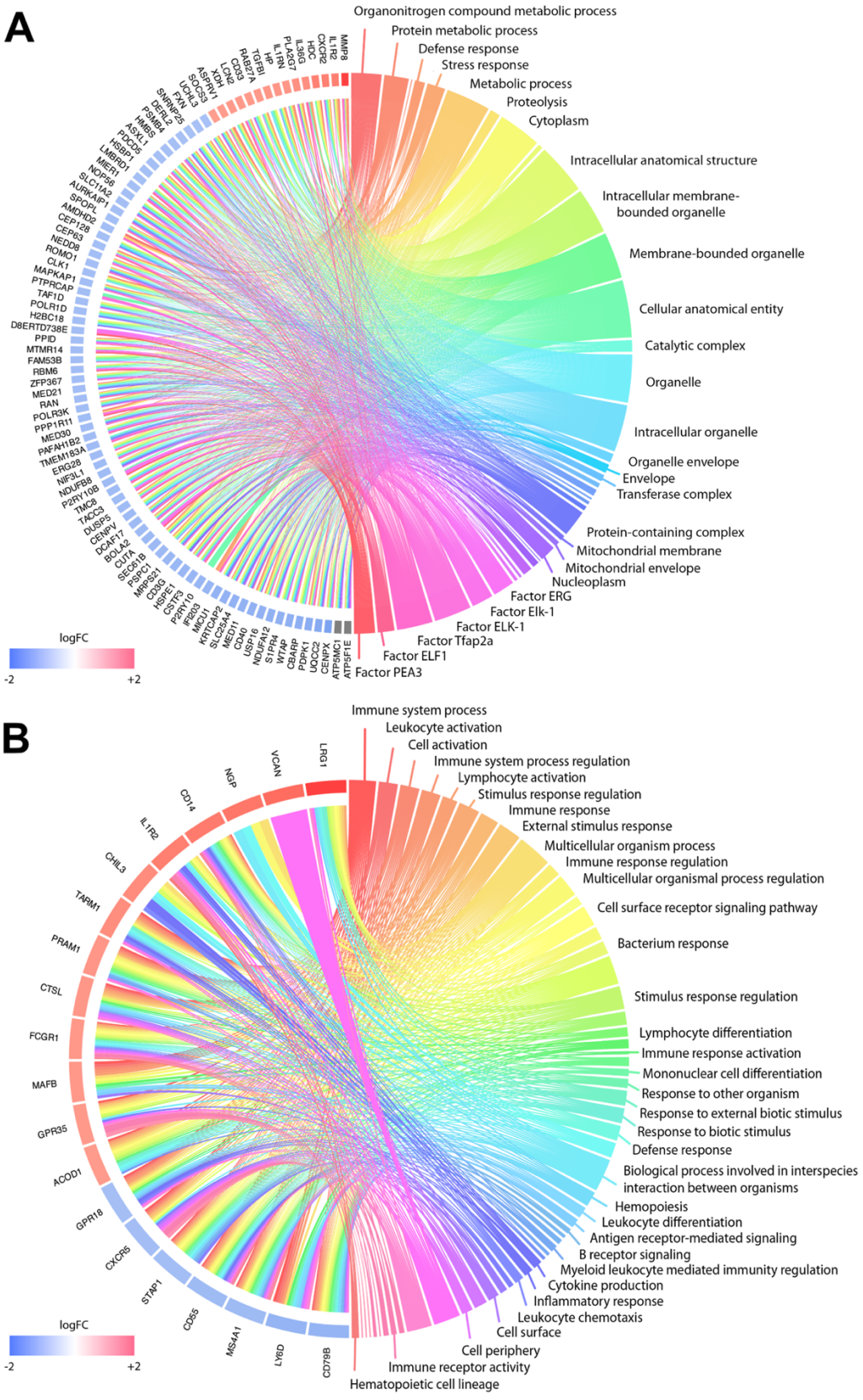
A
Organonitrogen compound metabolic process
Protein metabolic process
Defense response
Stress response
Metabolic process
Proteolysis
Cytoplasm
Intracellular anatomical structure
Intracellular membrane-bounded organelle
Membrane-bounded organelle
Cellular anatomical entity
Catalytic complex
Organelle
Intracellular organelle
Organelle envelope
Envelope
Transferase complex
Protein-containing complex
Mitochondrial membrane
Mitochondrial envelope
Nucleoplasm
Factor ERG
Factor Elk-1
Factor ELK-1
Factor Tfap2a
Factor ELF1
Factor PEA3
MMP8
IL1R2
CXCR2
HDC
IL36G
PLA2G7
IL1RN
HP
TGFBI
RAB27A
CD33
LCN2
XDH
ASPRV1
SOCS3
UCHL3
FXN
SNRNP25
DERL2
PSMB4
HMBS
ASXL1
PDCD5
HSBP1
LMBRD1
MIER1
NOP56
SLC11A2
AURKAIP1
SPOPL
AMDHD2
CEP128
CEP63
NEDD8
ROMO1
CLK1
MAPKAP1
PTPRCAP
TAF1D
POLR1D
H2BC18
D8ERTD738E
PPID
MTMR14
FAM53B
RBM6
ZFP367
MED21
RAN
POLR3K
PPP1R11
MED30
PAFAH1B2
TMEM183A
ERG28
NIF3L1
NDUFB8
P2RY10B
TMC8
TACC3
DUSP5
CENPV
DCAF17
BOLA2
CUTA
SEC61B
PSPC1
MRPS21
CD3G
HSPE1
CSTF3
P2RY10
IFI203
MICU1
KRTCAP2
SLC25A4
MED11
CD40
USP16
NDUFA12
S1PR4
WTAP
CBARP
PDPK1
UQCC2
CENPX
ATP5MC1
ATP5F1E
logFC
-2
+2
B
Immune system process
Leukocyte activation
Cell activation
Immune system process regulation
Lymphocyte activation
Stimulus response regulation
Immune response
External stimulus response
Multicellular organism process
Immune response regulation
Multicellular organismal process regulation
Cell surface receptor signaling pathway
Bacterium response
Stimulus response regulation
Lymphocyte differentiation
Immune response activation
Mononuclear cell differentiation
Response to other organism
Response to external biotic stimulus
Response to biotic stimulus
Defense response
Biological process involved in interspecies interaction between organisms
Hemopoiesis
Leukocyte differentiation
Antigen receptor-mediated signaling
B receptor signaling
Myeloid leukocyte mediated immunity regulation
Cytokine production
Inflammatory response
Leukocyte chemotaxis
Cell surface
Cell periphery
Immune receptor activity
Hematopoietic cell lineage
LRG1
VCAN
NGP
CD14
IL1R2
CHIL3
TARM1
PRAM1
CTSL
FCGR1
MAFB
GPR35
ACOD1
GPR18
CXCR5
STAP1
CD55
MS4A1
LY6D
CD79B
logFC
-2
+2

Figure 5. Gene ontology chord diagram showing core genes and significant pathways in **(A)** young and **(B)** aged MCAO+Recan mice. The diagram visualizes significant pathways on the right and their corresponding core genes on the left, with log fold change (logFC) indicated by coloured squares. Connections between the left (genes) and right (pathways) represent gene membership in a pathway's leading-edge subset. The gost() function was used to analyze gene ontology, utilizing gene identifiers from differential expression results. The analysis was conducted with Mus musculus as the organism, specifying evcodes=TRUE and significant=TRUE (p-value ≤ 0.05) to highlight relevant pathways and genes.

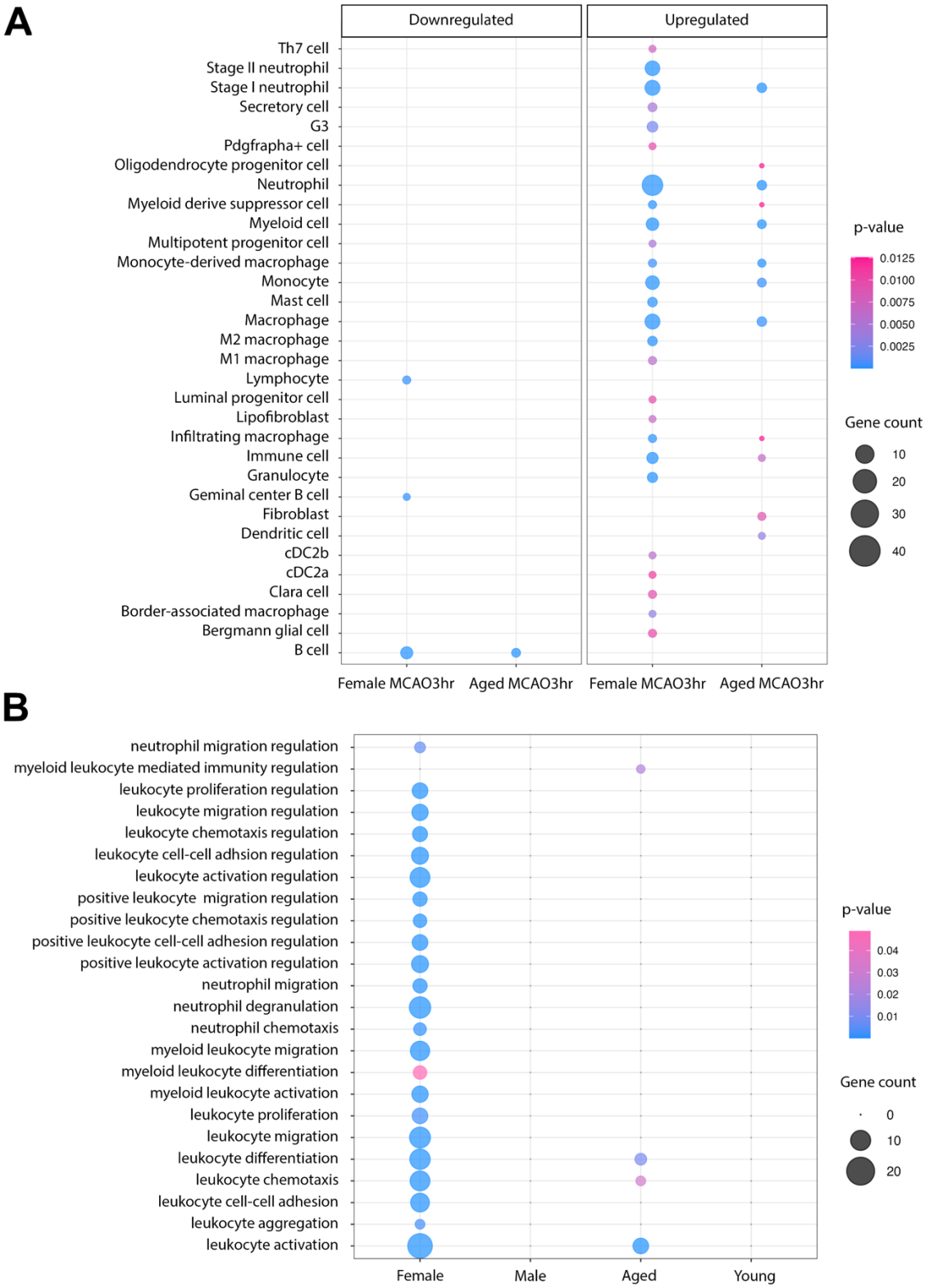

Figure 6 (A) Over-representation of cell markers from MCAO+Recan differentially expressed genes (DEGs). The Cell Marker 2.0 database and the clusterProfiler package were used to infer the cell types in which the identified DEGs might be expressed. The

dot plot shows upregulated and downregulated DEGs mapped to specific cell types. **(B)** Enrichment of leukocyte and neutrophil activities in female and aged MCAO+Recan mice. Gene enrichment analysis was conducted using the gProfiler package. The enrichplot::dotplot function was used to visualize enriched pathways, with colour intensity indicating the significance of enrichment and dot size representing the gene count for MCAO+Recan samples. These highlight the significant involvement of leukocyte and neutrophil activities in the ischemic stroke model.

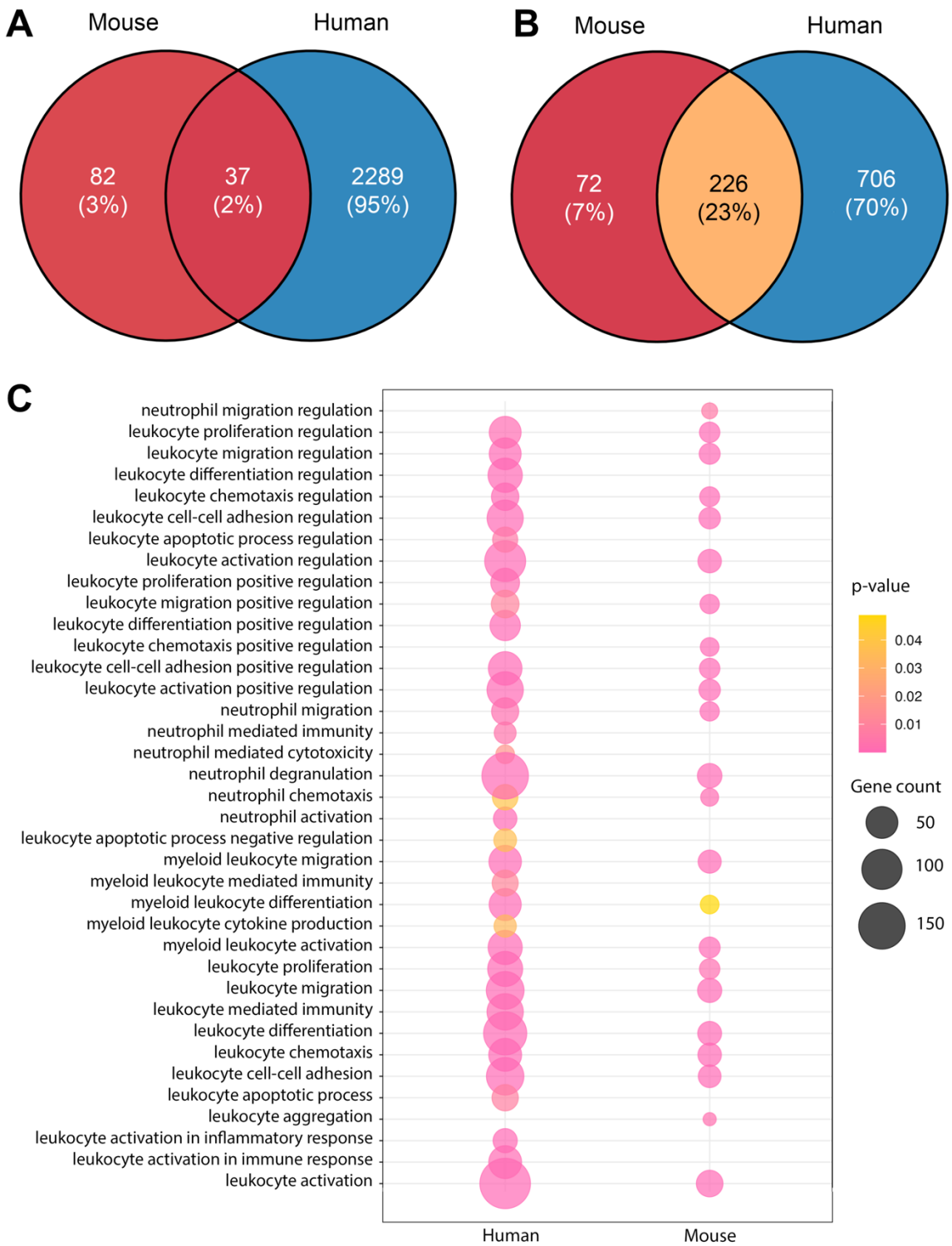

Figure 7 (A) Orthologue differentially expressed genes (DEGs) shared between MCAO+Recan female mice and clinical female patients. DEGs were identified in mouse and human datasets using the limma package ($|\log2FC| \geq 1.5$, p-value ≤ 0.05). The analysis highlights the common transcriptional responses to ischemic stroke and reperfusion (MCAO+Recan) across species. **(B)** Shared gene ontology (GO) terms and

KEGG pathways between MCAO+Recan mice and clinical patients. Functional enrichment analyses were performed using the gProfiler package to identify overlapping biological processes and pathways. Key shared pathways related to stroke, inflammation, and immune responses were identified, showing conserved functional responses across the species. **(C)** Conservation of leukocyte- and neutrophil-based pathways in human and mouse samples. Pathways related to leukocyte and neutrophil activity were conserved between human clinical patients and MCAO+Recan mice.

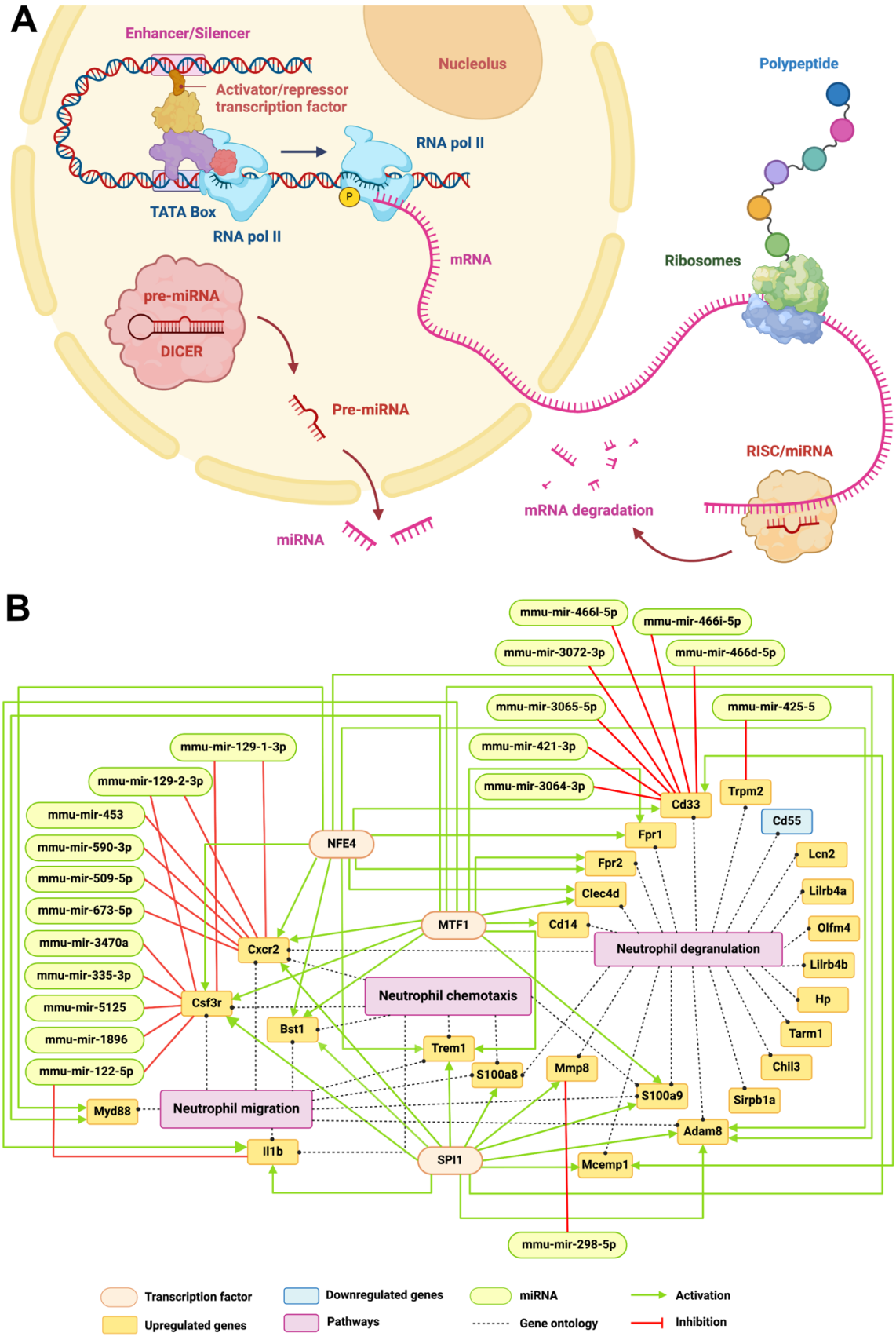
A
Enhancer/Silencer
Nucleolus
Polypeptide
Activator/repressor transcription factor
RNA pol II
TATA Box
RNA pol II
P
mRNA
Ribosomes
pre-miRNA
DICER
Pre-miRNA
RISC/miRNA
mRNA degradation
miRNA
B
mmu-mir-466l-5p
mmu-mir-466i-5p
mmu-mir-3072-3p
mmu-mir-466d-5p
mmu-mir-3065-5p
mmu-mir-425-5
mmu-mir-129-1-3p
mmu-mir-421-3p
mmu-mir-129-2-3p
mmu-mir-3064-3p
Cd33
Trpm2
mmu-mir-453
Cd55
NFE4
Fpr1
mmu-mir-590-3p
Lcn2
Fpr2
mmu-mir-509-5p
Lilrb4a
Clec4d
mmu-mir-673-5p
MTF1
Cd14
Olfm4
mmu-mir-3470a
Cxcr2
Neutrophil degranulation
Lilrb4b
mmu-mir-335-3p
Neutrophil chemotaxis
Hp
mmu-mir-5125
Csf3r
Bst1
Tarm1
mmu-mir-1896
Trem1
Chil3
mmu-mir-122-5p
S100a8
Mmp8
S100a9
Sirpb1a
Myd88
Neutrophil migration
Adam8
Il1b
SPI1
Mcemp1
mmu-mir-298-5p
Transcription factor
Downregulated genes
miRNA
Activation
Upregulated genes
Pathways
Gene ontology
Inhibition

Figure 8. (A) Transcriptional regulation by transcription factors (TFs) and miRNAs. mRNA is transcribed from DNA in the nucleus by the DNA polymerase II complex, a process regulated by TFs, which can act as activators or repressors. TFs bind to specific DNA regions, either enhancers or silencers, to increase or decrease gene transcription. In the cytoplasm, pre-miRNAs mature into miRNAs, which can cleave mRNA strands, destabilize mRNA, or inhibit translation. **(B)** Neutrophil signalling network. The neutrophil signalling network was generated using integrated results from gProfiler enrichment, NetworkAnalyst, and ChEA3 analyses. One TF can regulate several genes, and multiple TFs may regulate a single gene. Similarly, one gene can be regulated by multiple miRNAs, and each miRNA can target more than one gene. Graphs were created with BioRender.

Supplemental Material

Supplementary Table 1. Differential gene expression analysis from limma package of MCAO and MCAO+Recan ($|\log_2 FC| \geq 1.5$, p-value ≤ 0.05).

Group	Symbol	ID	Description	logFC	P Value	Adj P Val
MCAO	Plet1	76509	placenta expressed transcript 1	1.57	0.0018	0.2526
	Krt13	16663	keratin 13	1.56	0.0029	0.2757
	Psca	72373	prostate stem cell antigen	1.61	0.0013	0.2364
	Gsto1	14873	glutathione S-transferase omega 1	1.56	0.0043	0.2971
MCAO+Recan	Il1r2	16178	interleukin 1 receptor, type II	2.12	7.1091e-5	0.1261
	Cd55	13136	CD55 molecule, decay accelerating factor for complement	-1.58	3.0391e-4	0.1411
	Hdc	15186	histidine decarboxylase	1.68	9.1266e-4	0.1703
	Cd69	12515	CD69 antigen	-1.53	0.0014	0.1886
	Tarm1	245126	T cell-interacting, activating receptor on myeloid cells 1	1.57	0.0021	0.2015
	Mrgpra2a	668727	MAS-related GPR, member A2A	1.53	0.004	0.2363
	Mrgpra2b	235712	MAS-related GPR, member A2B	1.60	0.0036	0.2317
	Mt1	17748	metallothionein 1	1.52	0.0035	0.2292
	Mmp8	17394	matrix metallopeptidase 8	2.27	5.456e-4	0.1688
	Pou2af1	18985	POU domain, class 2, associating factor 1	-1.57	0.0011	0.1798
	Ngp	18054	neutrophilic granule protein	1.52	0.0149	0.3139
	Vcan	13003	versican	1.82	1.3353e-4	0.1262
	Ly6d	17068	lymphocyte antigen 6 complex, locus D	-1.79	4.6068e-5	0.0959
	H2-Oa	15001	histocompatibility 2, O region alpha locus	-1.57	2.4101e-5	0.0776
	Lrg1	76905	leucine-rich alpha-2-glycoprotein 1	2.32	9.2478e-4	0.1703
	Cd14	12475	CD14 antigen	1.50	0.0011	0.1795
	Ptprcap	19265	protein tyrosine phosphatase, receptor type, C polypeptide-associated protein	-1.62	1.8436e-6	0.0144
	Ms4a1	12482	membrane-spanning 4-domains, subfamily A, member 1	-1.54	5.133e-4	0.1650
	Ms4a6d	68774	membrane-spanning 4-domains, subfamily A, member 6D	1.87	0.0013	0.1846

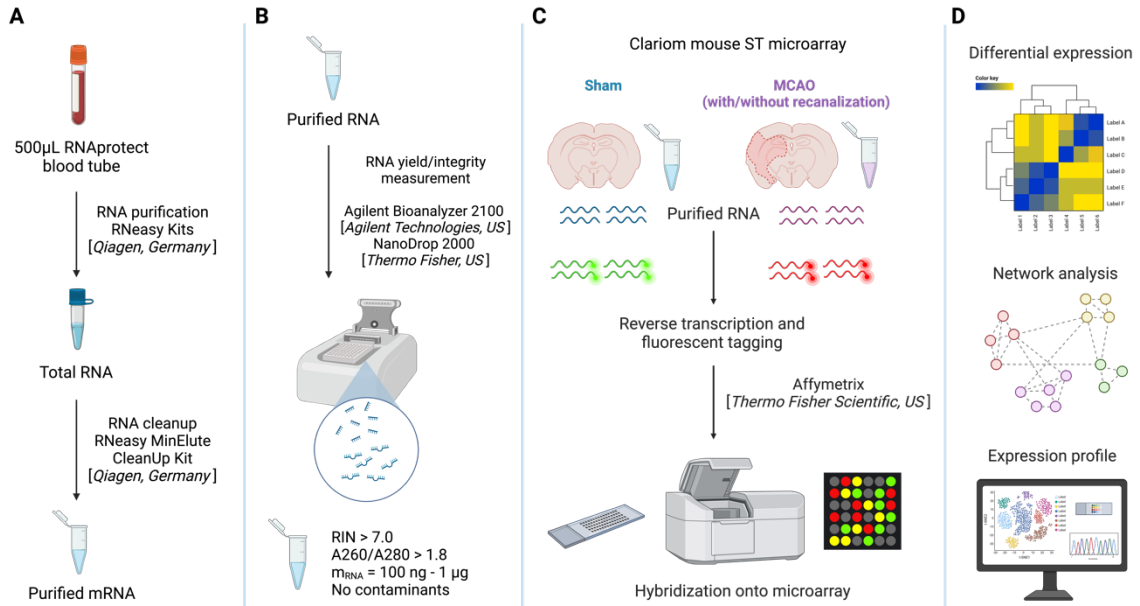

Supplementary Figure 1. Overview of RNA purification and microarray analysis procedures. **(A)** Sample collection and RNA extraction. Whole blood samples were obtained via retro-orbital sampling following sham and MCAO surgeries. Total RNA was extracted and purified using standardized QIAGEN protocols to ensure high-quality RNA for downstream analyses. **(B)** RNA selection for quality control. RNA samples were rigorously evaluated for yield and purity to ensure that only high-quality samples were used for microarray analysis. Stringent quality control measures were applied to select samples with optimal RNA integrity. **(C)** Microarray analysis using Affymetrix technology. Selected RNA samples were processed and analyzed on Affymetrix microarrays to generate comprehensive gene expression profiles. **(D)** Data normalization and differential expression analysis. Raw CEL files generated from the Affymetrix platform were normalized using robust statistical methods, followed by differential gene expression analysis with the limma package in RStudio. Enrichment analysis was performed using the gProfiler tool to identify biologically significant pathways enriched among the differentially expressed genes. These enriched pathways were subsequently visualized and interpreted using RStudio and Cytoscape to explore the molecular mechanisms underlying the gene expression changes.

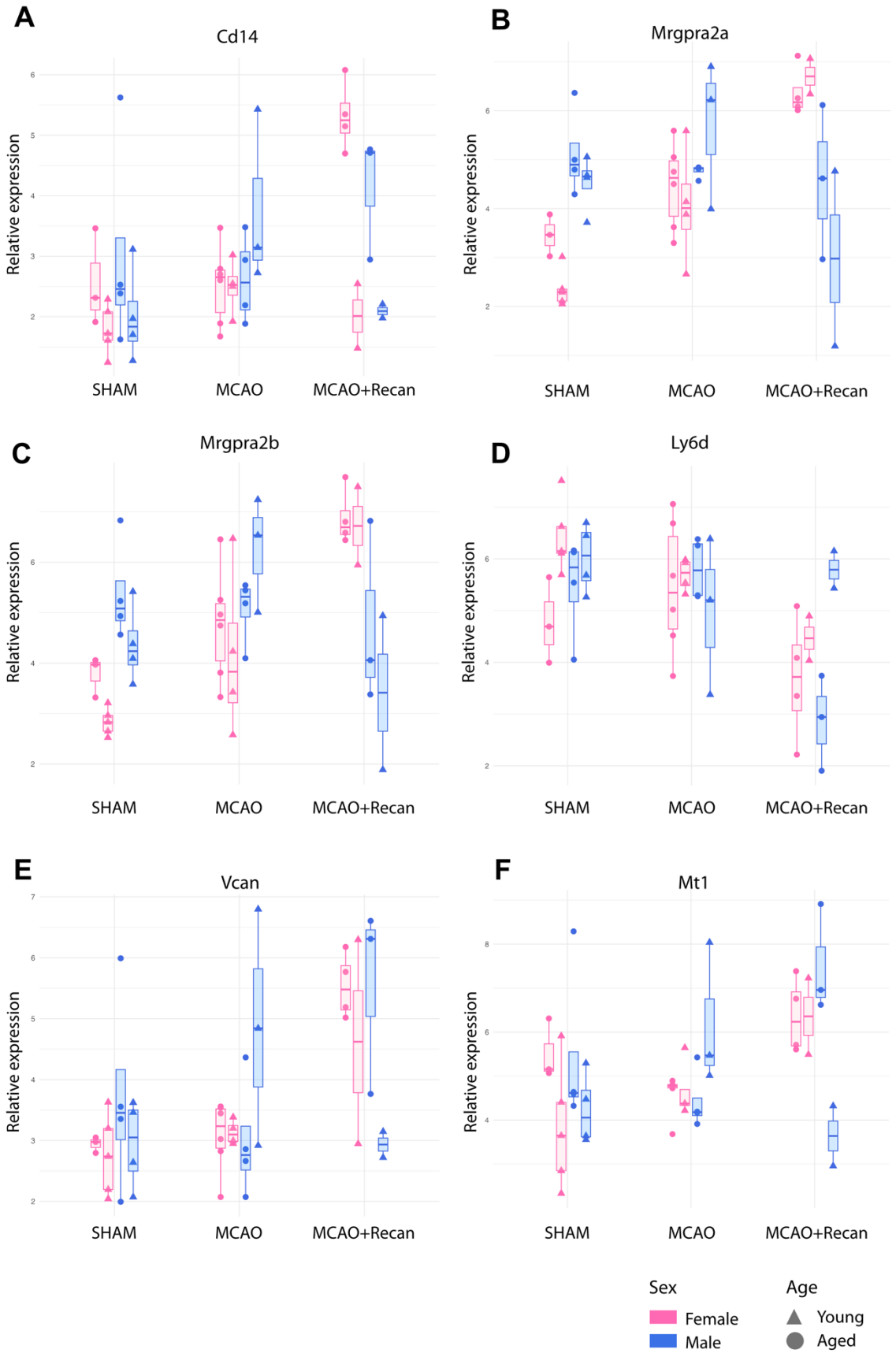
A
Cd14
B
Mrgpra2a
C
Mrgpra2b
D
Ly6d
E
Vcan
F
Mt1
Relative expression
SHAM
MCAO
MCAO+Recan
Sex
Female
Male
Age
Young
Aged

Supplementary Figure 2. Relative expression level of DEGs showing age- and sex-specific changes under different treatment methods (A) Cd14 **(B)** Mrgpra2a **(C)** Mrgpra2b **(D)** Ly6d **(E)** Vcan **(F)** Mt1 ($|\log_2 FC| \geq 1.5$, $p \leq 0.05$)

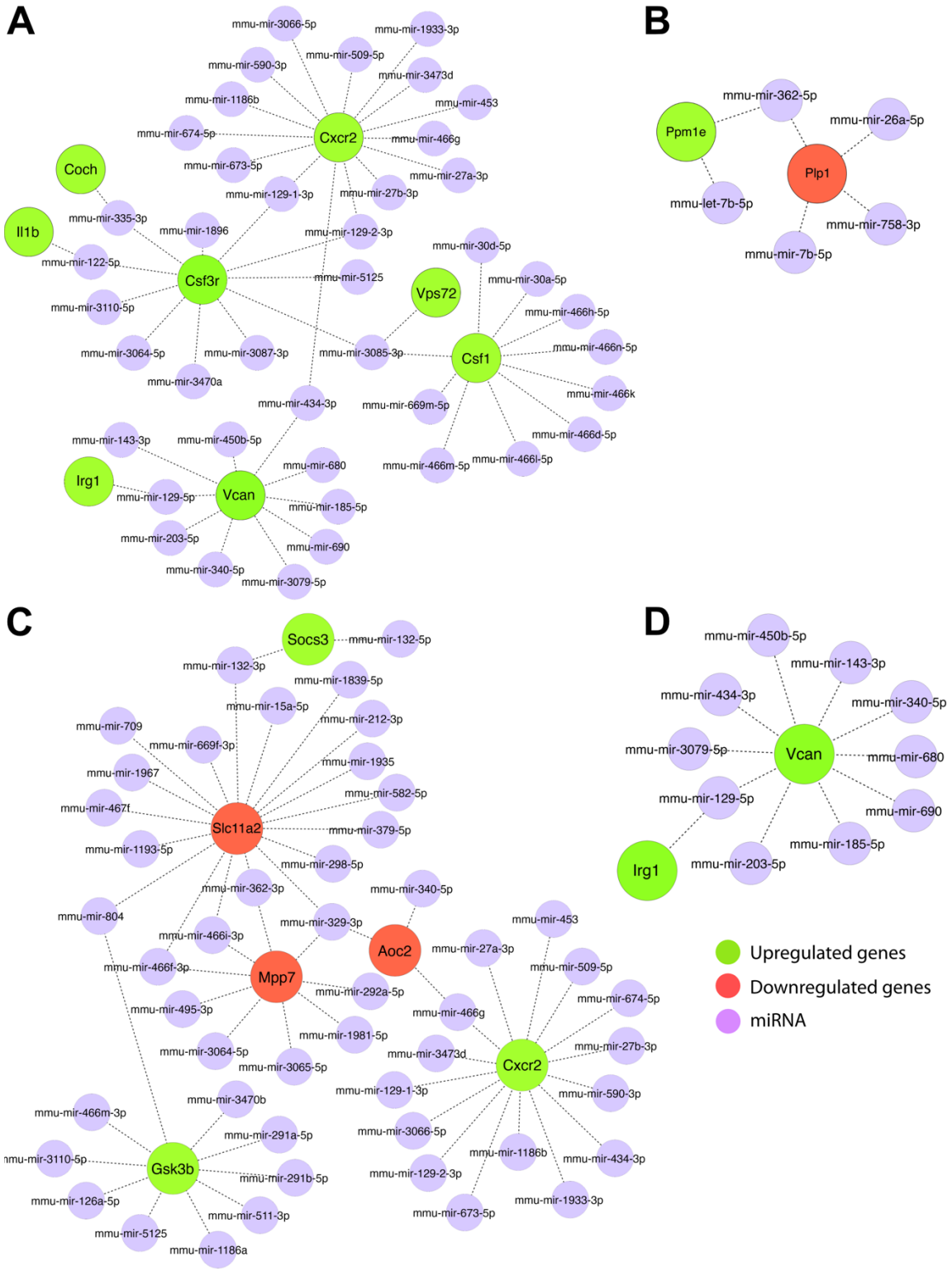

Supplementary Figure 3. miRNA-mRNA interactions in **(A)** female, **(B)** male, **(C)** young, and aged MCAO+Recan animals from NetworkAnalyst. One gene may be regulated by multiple miRNAs, and each miRNA can target more than one gene.

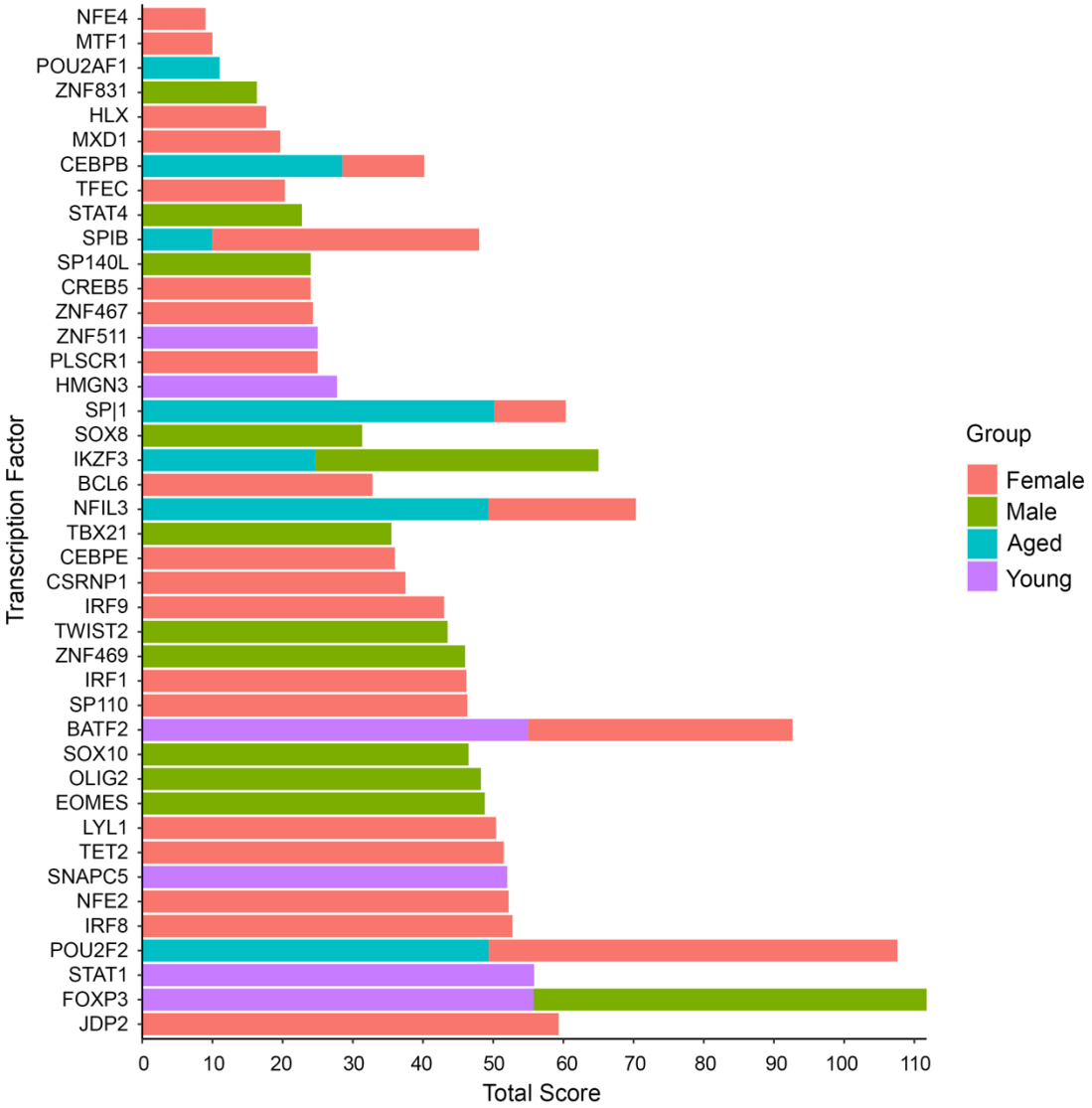

Supplementary Figure 4. Top 50 TFs identified by ChEA3. ChEA3 was used to predict TFs-mRNA regulatory network. Lists of DEGs of MCAO+Recans were submitted to the ChEA3 platform, and the top 50 TFs (organized by rank) were exported. One TF can regulate several genes, and multiple TFs may regulate one gene.